

Convergence rate analysis and improved iterations for numerical radius computation

Tim Mitchell*

January 31st, 2020

Revised: December 15th, 2020

Abstract

The current two main methods for computing the numerical radius are the level-set approach of Mengi and Overton and the cutting-plane method of Uhlig, but until now, no formal convergence rate results have been established for either. In practice, which is faster is also unclear, with Uhlig's method sometimes being much faster than Mengi and Overton's approach, and on other problems, much slower. In this paper, we clarify this issue and also propose three improved methods. We show that Mengi and Overton's method converges quadratically, as has been suspected, while we completely characterize the total cost of Uhlig's method for so-called disk matrices. Then, for arbitrary fields of values, we derive the exact Q-linear local convergence rate of Uhlig's cutting procedure. Together, this establishes that Uhlig's method is extremely expensive when the field of values is a disk centered at the origin, but that the local rate of convergence of his cutting procedure actually varies from linear to superlinear depending on the shape and location of the field of values, which we show can be encapsulated by a single parameter via introducing the notion of normalized curvature. These results fully explain why Uhlig's method can both be exceptionally fast and exceptionally slow. With this insight, we propose an improved level-set method and an improved cutting-plane method, both of which can be significantly faster than their earlier counterparts, while also establishing analogous convergence rate results for both. Moreover, in order to remain efficient for any field of values configuration, we introduce a third algorithm that leverages the concept of normalized curvature and combines both of our improved iterations.

Key words: field of values, numerical range and radius, transient behavior

Notation: $\|\cdot\|$ denotes the spectral norm, $\Lambda(\cdot)$ the spectrum (the set of eigenvalues) of a square matrix, and $\lambda_{\max}(\cdot)$ and $\lambda_{\min}(\cdot)$, respectively, the largest and smallest eigenvalue of a Hermitian matrix. e and i respectively denote Euler's number and $\sqrt{-1}$.

1 Introduction

For $A \in \mathbb{C}^{n \times n}$ and $x_k \in \mathbb{C}^n$, the trajectory of the discrete-time dynamical system

$$x_{k+1} = Ax_k \tag{1.1}$$

is clearly tied to powers of A , since $x_k = A^k x_0$ and so $\|x_k\| \leq \|A^k\| \|x_0\|$. As is well known, the asymptotic behavior of (1.1) is characterized by the moduli of the eigenvalues of A . Given the *spectral radius* of A ,

$$\rho(A) := \max\{|\lambda| : \lambda \in \Lambda(A)\}, \tag{1.2}$$

*Max Planck Institute for Dynamics of Complex Technical Systems, Magdeburg, 39106 Germany
`mitchell@mpi-magdeburg.mpg.de`.

$\lim_{k \rightarrow \infty} \|x_k\| = 0$ for all x_0 if and only if $\rho(A) < 1$, with the asymptotic decay rate being faster the closer $\rho(A)$ is to zero. However, if A is non-normal, its eigenvalues alone do not reveal the nature of the transient behavior of (1.1). Indeed, a central theme of Trefethen's and Embree's treatise on pseudospectra [TE05] is the very question of how large $\|A^k\|$ becomes before the asymptotic decay takes over.

One perspective is given by the *field of values (numerical range)* of A ,

$$W(A) := \{x^*Ax : x \in \mathbb{C}^n, \|x\| = 1\}, \quad (1.3)$$

as it imparts information about the transient behavior of (1.1). More specifically, consider the maximum of the moduli of points in $W(A)$, i.e., the *numerical radius*

$$r(A) := \max\{|z| : z \in W(A)\}. \quad (1.4)$$

It is known that $\frac{1}{2}\|A\| \leq r(A) \leq \|A\|$; see [HJ91, p. 44]. Combining the lower bound with the power inequality $r(A^k) \leq (r(A))^k$ [Ber65, Pea66] yields

$$\|A^k\| \leq 2(r(A))^k. \quad (1.5)$$

As $2(r(A))^k \leq \|A\|^k$ if and only if $r(A) \leq \sqrt[k]{0.5}\|A\|$, and $r(A) \leq \|A\|$ always holds, it follows that $2(r(A))^k$ is often a tighter upper bound for $\|A^k\|$ than $\|A\|^k$ is, and so the numerical radius can be useful in estimating the transient behavior of (1.1).¹

In 1996, Watson proposed two iterations akin to the power method for $r(A)$ [Wat96], the first of which converges at least to locally optimal approximations and a second simpler iteration that is less computationally intensive but lacks any convergence guarantees. However, as these iterations are so closely related to the power method, both may exhibit very slow convergence, and the cheaper iteration may not converge at all. Shortly thereafter [HW97], He and Watson combined Watson's cheaper iteration with a certificate test that was inspired by Byers' distance to instability algorithm [Bye88]. This certificate test either asserts that $r(A)$ has been attained (to a given tolerance) or provides a way of restarting Watson's cheaper iteration in order to aid convergence to $r(A)$; nevertheless, He and Watson's method is still not guaranteed to converge, due to Watson's cheaper iteration lacking convergence guarantees. In 2005, Mengi and Overton showed [MO05] that the certificate test of He and Watson actually enables an iteration guaranteed to converge to $r(A)$, namely an analogue of (the discrete-time variant of) the quadratically convergent level-set-based \mathcal{H}_∞ norm algorithm of Boyd, Balakrishnan, Bruinsma, and Steinbuch (BBBS) [BB90, BS90]. At each iteration, progress toward $r(A)$ is made by performing the certificate test, which computes all unimodular eigenvalues of a certain $2n \times 2n$ generalized eigenvalue problem. In practice, Mengi and Overton observed that their numerical radius method converged quadratically but did not prove this.

In 2009, Uhlig proposed a geometric approach to computing $r(A)$ [Uhl09] based on Johnson's earlier cutting-plane method for approximating the boundary of $W(A)$ [Joh78]. Johnson's method itself stems from the much earlier Bendixson-Hirsch theorem [Ben02] and fundamental results of Kippenhahn [Kip51]. Furthermore, in [Joh78, Remark 3], Johnson also mentioned that his algorithm could be adapted to compute the numerical radius but that a modified version might be more efficient. All of these geometric approaches are based on computing a number of supporting hyperplanes to sufficiently approximate the boundary of $W(A)$ or a region of it where $r(A)$ is attained. As obtaining these hyperplanes amounts to computing the largest eigenvalue of a sequence of $n \times n$ Hermitian matrices, by using sparse eigensolvers, these geometric-based algorithms can even be efficient for large-scale problems while still being globally convergent. Although Uhlig noted that the convergence of his method can sometimes be quite slow, no rate of convergence analysis appears to have been established for his method either. Nevertheless, Uhlig's experimental results showed his algorithm being decisively faster in practice than the apparently quadratically convergent method of Mengi and Overton.

¹Per [TE05], other quantities for assessing the transient behavior of (1.1) are the ε -*pseudospectral radius* and the *Kreiss constant* [Kre62]. For algorithms to compute these, see [MO05, BM19] and [Mit20, Mit19], respectively.

To shed light on this disparity, in this paper, we analyze both the algorithms of Mengi and Overton and of Uhlig, establishing the first rate-of-convergence results for these methods. Armed with our new insights, we also propose improved iterations for each. Our convergence rate analysis explains why Uhlig's cutting-plane method is sometimes much quicker than the level-set approach of Mengi and Overton on certain problems, while being much slower on others. Moreover, we use our new analysis to design a hybrid approach that remains efficient over all problems. The core idea, as we will establish in this paper, is the realization that the cost of any cutting-plane method is essentially determined by how closely, about the outermost points in the field of values, the boundary of the field of values resembles the circle of radius $r(A)$ centered at the origin. We characterize this resemblance by introducing the notion of *normalized curvature* using a parameter $\mu \in [0, 1]$, where 0 means no resemblance and 1 means exact agreement. If μ is close to 1, cutting-plane methods will be extremely expensive, but as μ becomes smaller, the linear rate of convergence of cutting-plane methods becomes quite fast and is in fact superlinear for $\mu = 0$. This insight, which enables our third algorithm that detects the normalized curvature and responds according, is beneficial since it allows the more efficient approach to be chosen automatically. This is particularly useful when minimizing the numerical radius of a parametrized matrix, where the numerical radius is computed for many different parameter choices, and so the shape and location of the field of values is constantly changing. Further underscoring the utility of this hybrid algorithm, per Lewis and Overton [LO20], numerical radius minimization problems often have solutions whose fields of values are disks centered at the origin, which correspond to $\mu = 1$.

The paper is organized as follows. We first give necessary preliminaries on the field of values, the numerical radius, and earlier algorithms for $r(A)$ in Section 2. Then in Section 3, we establish that Mengi and Overton's method does in fact converge quadratically and propose a faster improved level-set $r(A)$ algorithm, which also converges quadratically. We then analyze Uhlig's method in Section 4, deriving (a) its exact overall cost when the field of values is a disk centered at the origin, and (b) the precise Q-linear local rate of convergence of Uhlig's cutting procedure. In Section 5, we show how Uhlig's cutting procedure can be suboptimal and propose our second improved method using a more efficient cutting scheme, whose exact convergence rate we also derive. Making use of all these aforementioned results, we then describe our third and best algorithm in Section 6, validate our results experimentally in Section 7, and give concluding remarks in Section 8.

All experiments were done in MATLAB R2017b; the supplementary material contains code and the experimental setup to replicate all numerical results.

2 The field of values, the numerical radius, and earlier algorithms

We will need the following well-known facts about the field of values and the numerical radius; see [Kip51] and [HJ91, Chapter 1]. We generally assume that A is non-normal, as otherwise $r(A) = \rho(A)$, as seen in the following properties.

Remark 2.1. *Given $A \in \mathbb{C}^{n \times n}$,*

- (A1) *$W(A) \subset \mathbb{C}$ is a compact, convex set,*
- (A2) *if A is real, then $W(A)$ has real axis symmetry,*
- (A3) *if A is normal, then $W(A)$ is the convex hull of $\Lambda(A)$,*
- (A4) *$W(A) = [\lambda_{\min}(A), \lambda_{\max}(A)]$ if and only if A is Hermitian,*
- (A5) *the boundary of $W(A)$, $\partial W(A)$, is a piecewise smooth algebraic curve,*
- (A6) *if $v \in \partial W(A)$ is a point where $\partial W(A)$ is not differentiable, i.e., a corner, then $v \in \Lambda(A)$.
Corners always correspond to two line segments in $\partial W(A)$ meeting at some angle less than π radians.*

Definition 2.2. Given a nonempty closed set $\mathcal{D} \subset \mathbb{C}$, a point $\tilde{z} \in \mathcal{D}$ is (globally) outermost if $|\tilde{z}| = \max\{|z| : z \in \mathcal{D}\}$ and locally outermost if \tilde{z} is an outermost point of $\mathcal{D} \cap \mathcal{N}$, for some neighborhood \mathcal{N} of \tilde{z} .

For continuous-time systems $\dot{x} = Ax$, we have the *numerical abscissa*

$$\alpha_W(A) := \max\{\operatorname{Re} z : z \in W(A)\}, \quad (2.1)$$

i.e., the maximal real part of all points in $W(A)$. Unlike the numerical radius, computing the numerical abscissa is straightforward. In fact, all one needs to do is to compute the largest eigenvalue of a single Hermitian matrix [HJ91, p. 34]:

$$\alpha_W(A) = \lambda_{\max}\left(\frac{1}{2}(A + A^*)\right). \quad (2.2)$$

For $\theta \geq 0$, $W(e^{i\theta}A)$ is $W(A)$ rotated counter-clockwise about the origin. Consider

$$H(\theta) := \frac{1}{2}(e^{i\theta}A + e^{-i\theta}A^*), \quad (2.3)$$

so $\alpha_W(e^{i\theta}A) = \lambda_{\max}(H(\theta))$ and $\alpha_W(A) = \lambda_{\max}(H(0))$. For an angle θ , let λ_θ and x_θ denote, respectively, $\lambda_{\max}(H(\theta))$ and an associated normalized eigenvector. Furthermore, let L_θ denote the line $\{e^{-i\theta}(\lambda_\theta + it) : t \in \mathbb{R}\}$ and P_θ the half-plane $e^{-i\theta}\{z : \operatorname{Re} z \leq \lambda_\theta\}$ determined by line L_θ . Then P_θ is a *supporting hyperplane* for $W(A)$ with the following properties: [Joh78, p. 597]

(B1) $W(A) \subseteq P_\theta$ for all $\theta \in [0, 2\pi)$,

(B2) $b_\theta = x_\theta^* A x_\theta \in \partial W(A) \cap L_\theta$, i.e., L_θ is tangent² to $\partial W(A)$ at $b_\theta \in \mathbb{C}$,

(B3) $W(A) = \cap_{\theta \in [0, 2\pi)} P_\theta$.

As $H(\theta + \pi) = -H(\theta)$, $P_{\theta + \pi}$ can alternatively be obtained via the smallest eigenvalue of $H(\theta)$ and its associated eigenvector. The Bendixson-Hirsch theorem is a special case of these properties, defining the bounding box (with sides parallel to the axes) of $W(A)$, for $\theta = 0$ and $\theta = \frac{\pi}{2}$.

Definition 2.3. Let $b \in \partial W(A)$. If b is a point where $\partial W(A)$ is smooth, then the radius of curvature \tilde{r} of $\partial W(A)$ at b is the radius of the osculating circle of $\partial W(A)$ at b , i.e., the circle with the same tangent and curvature \tilde{r} of $\partial W(A)$ at b . If b is a corner, we say that the radius of curvature $\tilde{r} = 0$, while if $\partial W(A)$ is a line segment in a neighborhood of b , then $\tilde{r} = \infty$.

Key Remark 2.4. An important property of osculation is that if a curve C is twice differentiable at a point p , then C and its osculating circle have second or higher order contact at p , i.e., their disagreement decays at least cubically as p is approached; see, e.g., [Küh15, chapter 2]. Per (A5) and (A6), $\partial W(A)$ is infinitely differentiable at any $b \in \partial W(A)$ that is not a corner. Thus, for any non-corner $b \in \partial W(A)$, the osculating circle is a second-order (or better) local approximation of $\partial W(A)$ about b .

In [Fie81, Theorem 3.3], Fiedler derived a formula to compute the radius of curvature of $\partial W(A)$ at a given boundary point based on $\lambda_{\max}(H(\theta))$ and its associated normalized eigenvector. However, this result assumes that $\lambda_{\max}(H(\theta))$ is a simple eigenvalue, which may not always hold.

Via (2.2) and (2.3), the numerical radius can be written as

$$r(A) = \max_{\theta \in [0, 2\pi)} h(\theta) \quad \text{where} \quad h(\theta) := \lambda_{\max}(H(\theta)), \quad (2.4)$$

i.e., a one-variable maximization problem. Via $H(\theta + \pi) = -H(\theta)$, it also follows that

$$r(A) = \max_{\theta \in [0, \pi)} \rho(H(\theta)). \quad (2.5)$$

²If b_θ is a corner of $\partial W(A)$, L_θ might be better described as a supporting line of $\partial W(A)$, since $\partial W(A)$ is not differentiable at b_θ and $W(A)$ has more than one supporting hyperplane at b_θ . However, for simplicity, we always refer to L_θ as a tangent line and b_θ as a tangential boundary point.

However, as (2.4) and (2.5) may have multiple maxima (possibly infinitely many, if $W(A)$ is a disk centered at the origin), it is not straightforward to find a global maximizer of either, and crucially, assert that it is indeed a global maximizer in order to verify that $r(A)$ has been computed.

While Watson's first iteration converges to local maximizers of (2.5), it was his second iteration (that is not guaranteed to converge) that He and Watson employed with their certificate test to estimate $r(A)$, due to it being much cheaper (though both require $\mathcal{O}(n^2)$ work per iteration). Whenever this so-called “simple iteration” terminates or stagnates (e.g., due to slow convergence), their certificate test either asserts that $r(A)$ has in fact been attained (to a tolerance), or it restarts the simple iteration in a monotonic way, so that more progress toward $r(A)$ hopefully can be made in the next round. Given $\gamma \in \mathbb{R}$, Mengi and Overton noted that the certificate test can also be used to obtain all the γ -level set points (if any) of $h(\theta)$, i.e., $\{\theta : h(\theta) = \gamma\}$, which they then used to develop an analogue of the BBBS \mathcal{H}_∞ -norm algorithm for estimating $r(A)$ via (2.4). Given $\gamma_j \leq r(A)$, the certificate test computes all intervals under $h(\theta)$ whose endpoints are in the γ_j -level set of $h(\theta)$. Then $h(\theta)$ is evaluated at the midpoints of these intervals, and γ_{j+1} is set to the highest of the corresponding function values. This process is done in a loop, with the sequence $\{\gamma_j\} \rightarrow r(A)$ monotonically. Mengi and Overton stated that they believed quadratic convergence of their iteration could be shown via a similar argument to that done for the BBBS algorithm in [BB90], although they did not pursue this [MO05, p. 667].

The certificate (or level-set) test is based on [MO05, Theorem 3.1], which is a slight restatement of [HW97, Theorem 2] from He and Watson. We omit the proof.

Theorem 2.5. *Given $\gamma \in \mathbb{R}$, the pencil $R_\gamma - \lambda S$ has $e^{i\theta}$ as an eigenvalue or is singular if and only if γ is an eigenvalue of $H(\theta)$ defined in (2.3), where*

$$R_\gamma := \begin{bmatrix} 2\gamma I & -A^* \\ I & 0 \end{bmatrix} \quad \text{and} \quad S := \begin{bmatrix} A & 0 \\ 0 & I \end{bmatrix}. \quad (2.6)$$

The γ -level set of $h(\theta) = \lambda_{\max}(H(\theta))$ is associated with the unimodular eigenvalues of $R_\gamma - \lambda S$, but the converse is not true, i.e., for a unimodular eigenvalue of $R_\gamma - \lambda S$, γ may correspond to an eigenvalue of $H(\theta)$ other than $\lambda_{\max}(H(\theta))$. Furthermore, $R_\gamma - \lambda S$ is always nonsingular for all $\gamma > h(\theta)$, for any $\theta \in [0, 2\pi)$. This is because if $W(A)$ and a disk centered at the origin enclosing $W(A)$ have more than n shared boundary points, then $W(A)$ is that disk; see [TY99, Lemma 6]. The downside to the BBBS-like iteration is that it does cubic work per iteration with a significant constant factor, as all unimodular eigenvalues of $R_\gamma - \lambda S$ must be computed for each $\gamma = \gamma_j$,

Uhlig's algorithm, on the other hand, computes the numerical radius via refining

$$\mathcal{P}_j := \bigcap_{\overline{\theta} \in \{\overline{\theta}_1, \dots, \overline{\theta}_j\}} P_{\overline{\theta}} \quad (2.7)$$

a convex polygonal approximation of $W(A)$, i.e., the intersection of supporting hyperplanes for angles $\{\overline{\theta}_1, \dots, \overline{\theta}_j\}$. For clarity, for the remainder of this paper, we will always use an overline to denote any angle specifying a supporting hyperplane, i.e., $P_{\overline{\theta}}$, while θ , without an overline, will be used to denote angles in all other contexts. For any (closed) approximation \mathcal{P}_j , the following properties hold:

- (C1) $W(A) \subseteq \mathcal{P}_j$ and so \mathcal{P}_j is an overapproximation of $W(A)$,
- (C2) $|b| \leq r(A)$ holds for any tangential boundary point $b \in \partial W(A) \cap \mathcal{P}_j$,
- (C3) $r(A) \leq |c_j|$, where c_j is an outermost corner of the polygon \mathcal{P}_j .

Thus, \mathcal{P}_j provides the following upper bound and relative error for $r(A)$:

$$r_{\text{ub}}(A; \mathcal{P}_j) := \max\{|c| : c \text{ an outermost of } \mathcal{P}_j\} \geq r(A), \quad (2.8a)$$

$$r_{\text{err}}(A; \mathcal{P}_j) := \frac{r_{\text{ub}}(A; \mathcal{P}_j) - r(A)}{r(A)}. \quad (2.8b)$$

By sufficiently refining the outermost corners of \mathcal{P}_j , so that for some $k \geq j$ we have that $r_{\text{err}}(A; \mathcal{P}_k)$ falls below some desired tolerance, $r(A)$ can be computed to any desired accuracy. Uhlig's method achieves this via a greedy strategy. On each iteration, his algorithm attempts to chop off an outermost corner c_j from \mathcal{P}_j , by adding the supporting hyperplane for $\bar{\theta}_{j+1} = -\text{Arg}(c_j)$ to create \mathcal{P}_{j+1} . If c_j happens to be a corner of $\partial W(A)$, then this operation asserts that $|c_j| = r(A)$ and the computation is done. Otherwise, $c_j \notin W(A)$ and the addition of the supporting hyperplane for $\bar{\theta}_{j+1} = -\text{Arg}(c_j)$ prunes corner c_j from \mathcal{P}_j to yield \mathcal{P}_{j+1} , a smaller polygonal region, and $r_{\text{err}}(A; \mathcal{P}_{j+1}) \leq r_{\text{err}}(A; \mathcal{P}_j)$ (strictly less if there were no ties for the outermost corner of \mathcal{P}_j). Meanwhile, this cutting operation also adds a new tangential boundary point b_{j+1} , where $b_{j+1} = x_{j+1}^* A x_{j+1}$ and x_{j+1} is the eigenvector for $\lambda_{\max}(H(\bar{\theta}_{j+1}))$. Figure 1 depicts Uhlig's method when a corner is cut.

Remark 2.6. *If $\lambda_{\min}(H(\bar{\theta}_{j+1}))$ and its eigenvector are computed, then \mathcal{P}_j can also be refined for the parallel supporting hyperplane on the other side of $W(A)$, i.e., the one with angle $\pi - \text{Arg}(c_j)$. Whether this will be useful is not necessarily clear a priori, but if λ_{\min} can be obtained with negligible addition cost, there is little reason not to also do this second refinement. For all but the smallest n , Uhlig's `NumRadius` routine, which implements his method in MATLAB, only does single refinements using λ_{\max} .*

Compared to computing $r(A)$ via Johnson's $\partial W(A)$ algorithm, Uhlig's greedy method is generally more efficient as it only needs to sufficiently approximate $\partial W(A)$ in the regions where $r(A)$ is attained. However, if $W(A)$ is a disk centered at the origin, then $r(A)$ is attained at every boundary point, and so Uhlig's method, like Johnson's, must approximate all of $\partial W(A)$. Such *disk matrices*, i.e., those whose field of values are circular disks centered at the origin, are relatively rare but can arise from optimizing the numerical radius of certain parametrized matrices; see [LO20] for a thorough discussion. One particular example of a disk matrix, whose history and relevance is described in [LO20, section 4], is the $n \times n$ Crabb matrix:

$$K_2 = \begin{bmatrix} 0 & 2 \\ 0 & 0 \end{bmatrix}, \quad K_3 = \begin{bmatrix} 0 & \sqrt{2} & 0 \\ 0 & 0 & \sqrt{2} \\ 0 & 0 & 0 \end{bmatrix}, \quad K_n = \begin{bmatrix} 0 & \sqrt{2} & & & \\ & \ddots & 1 & & \\ & & \ddots & \ddots & \\ & & & \ddots & 1 \\ & & & & \sqrt{2} \\ & & & & 0 \end{bmatrix}, \quad (2.9)$$

where $r(K_n) = 1$ for all n , i.e., its field of values is always the unit disk.

Finally, Uhlig discussed how Chebfun [DHT14], a software package for approximating functions via interpolation, can be used to compute $r(A)$ with just a few lines of MATLAB, but that is often orders of magnitude slower than either his cutting-plane method or the algorithm of Mengi and Overton; see [Uhl09, Section 3].

3 Quadratic convergence and improvements to the level-set approach

For computing the \mathcal{H}_∞ norm, Boyd and Balakrishnan established that the BBBS method converges at least quadratically, stating that the result was “a direct consequence of the regularity result in Theorem 2.3” [BB90, p. 6], where regularity in this context means that the function being maximized is twice continuously differentiable at maximizers. In the context of the \mathcal{H}_∞ norm, the function being maximized is the norm of the transfer function along the imaginary axis, while in Mengi and Overton's $r(A)$ method, it is $h(\theta)$ from (2.4). Thus, to show that the quadratic convergence of Boyd and Balakrishnan does extend to Mengi and Overton's method, it suffices to show that $h(\theta)$ is twice continuously differentiable at maximizers,³ which we now do.

³For brevity, we do this for global maximizers, but Theorem 3.1 can be rewritten for local ones.

Theorem 3.1. *If A is a disk matrix, $h(\theta) = \rho(H(\theta)) = r(A)$ for all $\theta \in (-\pi, \pi]$. Otherwise, recalling Definition 2.3 for curvature, for any outermost point b_* in $W(A)$, i.e., $|b_*| = r(A)$, in a neighborhood about $\theta = -\text{Arg}(b_*)$ either*

- (i) b_* is a corner and $h(\theta) = r(A) \cos \theta$ or
- (ii) $h(\theta) = (r(A) - \tilde{r}) \cos \theta + \tilde{r} + \mathcal{O}(\theta^3)$, where $\tilde{r} > 0$ is the curvature of $\partial W(A)$ at b_* .

Claims (i) and (ii) also hold when $h(\theta)$ is replaced by $\rho(H(\theta))$ if $b_\pi := r(A)e^{i(\pi-\theta)}$ is not also an outermost point of $W(A)$. However, if $b_\pi \in W(A)$ as well, then either

- (iii) b_* and b_π are both corners and $\rho(H(\theta)) = r(A) \cos \theta$ or
- (iv) $\rho(H(\theta)) = (r(A) - \tilde{r}) \cos \theta + \tilde{r} + \mathcal{O}(\theta^3)$, where $\tilde{r} > 0$ is the larger of the two curvatures of $\partial W(A)$ at b_* and b_π .

Proof. If A is a disk matrix, $W(A)$ is a disk centered at the origin, and so $h(\theta)$ is constant, specifically $r(A)$. Otherwise, b_* is an outermost point of $W(A)$ if and only if $h(-\text{Arg}(b_*)) = r(A)$, and there are at most n of these global maximizers. Let b_* be any one of these outermost points. Without loss of generality, we can assume that $\text{Arg}(b_*) = 0$, and so b_* is also a rightmost point of $W(A)$ with $h(0) = r(A)$. This rightmost point must be unique since if there were to exist a tie, i.e., $b \in W(A)$ with $\text{Re } b = \text{Re } b_*$ but $\text{Im } b \neq \text{Im } b_* = 0$, then $|b| > |b_*|$, which contradicts the assumption that b_* is an outermost point. If b_* is a corner (or the end of the line segment $W(A)$ when A is Hermitian), then $P_{\overline{\theta}}$ is a supporting hyperplane of $W(A)$ for all $\overline{\theta}$ in some neighborhood \mathcal{N} about 0. Thus, for $\theta \in \mathcal{N}$, $e^{i\theta}b_*$ is a rightmost point of $W(e^{i\theta}A)$, and $\alpha_W(e^{i\theta}A) = h(\theta) = \text{Re } e^{i\theta}b_*$, proving (i). Otherwise, if b_* is not a corner, it must be a boundary point where $\partial W(A)$ is smooth by (A5) and (A6). Per Key Remark 2.4, the osculating circle of $\partial W(A)$ at b_* , which has radius $\tilde{r} > 0$ and center $r(A) - \tilde{r}$, agrees with $\partial W(A)$ to at least second order about b_* . Hence, the rightmost point of this osculating circle as it is rotated about the origin agrees with the rightmost point of $W(e^{i\theta}A)$ to at least second order in a neighborhood about $\theta = 0$, and so (ii) then follows via a simple trigonometric argument. Since $\rho(H(\theta)) = \max\{h(\theta), h(\theta + \pi)\}$, the entire proof applies analogously to obtain (i)–(iv). \square

We now propose two straightforward but important modifications to make the level-set approach faster and more reliable. We need the following immediate corollary of Theorem 2.5.

Corollary 3.2. *Given $\gamma \geq 0$, if $\rho(H(\theta)) = \gamma$, then there exists a $\lambda \in \mathbb{C}$ such that $|\lambda| = 1$, $\det(R_\gamma - \lambda S) = 0$, and $\theta = a(\text{Arg}(\lambda))$, where $a : (-\pi, \pi] \mapsto [0, \pi)$ is*

$$a(\theta) := \begin{cases} \theta + \pi & \text{if } \theta < 0 \\ 0 & \text{if } \theta = 0 \text{ or } \theta = \pi \\ \theta & \text{otherwise.} \end{cases} \quad (3.1)$$

First, as clarified by Corollary 3.2, Theorem 2.5 actually allows all points in any γ -level set of either $h(\theta)$ or $\rho(H(\theta))$ to be computed, and so one should in fact do a BBBS-like iteration using (2.5) instead of (2.4). Per Theorem 3.1, this modified iteration will also have local quadratic convergence, but using $\rho(H(\theta))$ can also be faster in practice than Mengi and Overton's $h(\theta)$ -based method. This is because $\rho(H(\theta)) \geq h(\theta)$ always holds, $\rho(H(\theta)) \geq 0$ (unlike $h(\theta)$, which can be negative), and the optimization domain is reduced from $[0, 2\pi)$ to $[0, \pi)$. Thus, every level-set update γ_j computed via (2.5) must be at least as good and possibly much better than that of working with (2.4), and there may also be fewer level-set intervals per iteration, all of which can reduce the overall cost in a meaningful way.

Second, one should also use local optimization on top of the BBBS-like step at every iteration, i.e., the BBBS-like step is used to initialize optimization in order to find a maximizer of (2.5). The first benefit is speed, as optimization generally results in much larger updates to γ_j and

these updates are now locally optimal. This greatly reduces the total number of expensive eigenvalue computations done with $R_\gamma - \lambda S$, often down to just one. The overall runtime is also greatly lowered because optimization is relatively cheap (as we explain momentarily). The second benefit is that using optimization also avoids some numerical difficulties when solely working with $R_\gamma - \lambda S$ to update γ_j . In their 1997 paper, He and Watson showed that the condition number of a unimodular eigenvalue of $R_\gamma - \lambda S$ actually blows up as θ approaches critical values of $h(\theta)$ or $\rho(H(\theta))$ [HW97, Theorem 4],⁴ as this corresponds to a pair of unimodular eigenvalues of $R_\gamma - \lambda S$ coalescing into a double eigenvalue. Since this must occur as $\{\gamma_k\} \rightarrow r(A)$, rounding errors may prevent the relevant pair of eigenvalues from being detected, causing such level-set algorithms to stagnate before attaining $r(A)$ to the desired accuracy. He and Watson even stated that their analytical result was “hardly encouraging” [HW97, p. 336], even though they did not observe this issue in their experiments. However, an example of such a deleterious effect is shown in [BM19, Figure 2], where analogous eigenvalue computations are shown to greatly reduce numerical accuracy when computing the *pseudospectral abscissa* [BLO03].

In contrast, $\rho(H(\theta))$ is, per Theorem 3.1, rather nicely behaved at maximizers, Lipschitz since $H(\theta)$ is Hermitian (see, e.g., [Kat82, Theorem II.6.8]), and its value and derivatives are relatively cheap to compute. Thus, local optimizers of (2.5) can be obtained using, say, Newton’s method, with only a handful of iterations. In fact, in their concluding remarks [HW97, p. 341–2], He and Watson even mention that their use of Watson’s simple iteration could be replaced with Newton’s method, since it has faster local convergence (quadratic). However, they seemingly dismissed this idea by claiming there would be “a considerable increase in computation” due to the costs of obtaining first and second derivatives of $\rho(H(\theta))$ and the need for a line search. Actually, as we explain below, the cost to compute these derivatives is typically negligible. Furthermore, for large-scale problems, only the second derivative becomes expensive to compute, but in this case, one can use the secant method, which still has fast local convergence (superlinear) and only requires first derivatives. Finally, with either Newton’s or the secant method, steps of length one are eventually accepted; hence, the cost of line searches is not a critical concern in terms of overall efficiency.

Remark 3.3. *While other techniques, e.g., subspace methods, might be used to find maximizers of $h(\theta)$ or $\rho(H(\theta))$, the point we make here is that standard optimization is already so effective that there is little practical reason to consider alternatives.*

Let λ_j be an eigenvalue whose modulus attains $\rho(H(\theta))$ with x_j its corresponding normalized eigenvector, and assume λ_j is unique (so $j = 1$ or $j = n$ when the spectrum of $H(\theta)$ is sorted). By standard perturbation theory for eigenvalues,

$$\rho'(H(\theta)) = \text{sgn}(\lambda_j) \cdot x_j^* H'(\theta) x_j = \text{sgn}(\lambda_j) \cdot x_j^* \left(\frac{i}{2} (e^{i\theta} A - e^{-i\theta} A^*) \right) x_j. \quad (3.2)$$

Thus, given λ_j and x_j , the additional cost of obtaining $\rho'(H(\theta))$ mostly amounts to the single matrix-vector product $H'(\theta)x_j$. To compute $\rho''(H(\theta))$, we will need the following result for second derivatives of eigenvalues; see [Lan64, OW95].

Theorem 3.4. *For $t \in \mathbb{R}$, let $A(t)$ be a twice-differentiable $n \times n$ Hermitian matrix family with, for $t = 0$, eigenvalues $\lambda_1 \geq \dots \geq \lambda_n$ and associated eigenvectors x_1, \dots, x_n , with $\|x_k\| = 1$ for all k . Then assuming λ_j is unique,*

$$\lambda_j''(t) \Big|_{t=0} = x_j^* A''(0) x_j + 2 \sum_{k \neq j} \frac{|x_k^* A'(0) x_j|^2}{\lambda_k - \lambda_j}.$$

Although obtaining the eigendecomposition of $H(\theta)$ is cubic work, this is generally negligible compared to the cost of obtaining all the unimodular eigenvalues of $R_\gamma - \lambda S$, which is necessary to use Theorem 2.5; recall that $H(\theta)$ is an $n \times n$ Hermitian matrix, while $R_\gamma - \lambda S$ is a $2n \times 2n$

⁴The exact statement appears in the last lines of the corresponding proof on p. 335.

Algorithm 1 An Improved Level-Set Algorithm

Input: $A \in \mathbb{C}^{n \times n}$, initial guesses $\mathcal{M} = \{\theta_1, \dots, \theta_q\}$, and tolerance $\tau_{\text{tol}} > 0$.
Output: γ such that $|\gamma - r(A)| \leq \tau_{\text{tol}} \cdot r(A)$.

```

1:  $\theta_0 \leftarrow a(\text{Arg}(\lambda))$  where  $\lambda \in \Lambda(A)$  such that  $|\lambda| = \rho(A)$  // 0 if  $\lambda = 0$ 
2:  $\mathcal{M} \leftarrow \mathcal{M} \cup 0 \cup \theta_0$ 
3: while  $\mathcal{M}$  is not empty do
4:    $\theta_{\text{BBBS}} \leftarrow \arg \max_{\theta \in \mathcal{M}} \rho(H(\theta))$  // In case of ties, just take any one
5:    $\gamma \leftarrow$  maximization of  $\rho(H(\theta))$  via local optimization initialized at  $\theta_{\text{BBBS}}$ 
6:    $\gamma \leftarrow \gamma(1 + \tau_{\text{tol}})$ 
7:    $\mathcal{T}_{\text{RS}} \leftarrow \{a(\text{Arg } \lambda) : \det(R_\gamma - \lambda S) = 0, |\lambda| = 1\}$ 
8:    $\{\theta_1, \dots, \theta_q\} \leftarrow \mathcal{T}_{\text{RS}}$  sorted in increasing order with any duplicates removed
9:    $\mathcal{M} \leftarrow \{\theta : \rho(H(\theta)) > \gamma \text{ where } \theta = 0.5(\theta_k + \theta_{k+1}), k = 1, \dots, q - 1\}$ 
10: end while

```

NOTE: For simplicity, we forgo giving pseudocode to describe optimizations that exploit symmetry of $W(A)$ and assume here that all eigenvalues are obtained exactly. Recall that $a(\cdot)$ is defined in (3.1), and note that the method reduces to a BBBS-like iteration using (2.5) if line 5 is replaced with $\gamma \leftarrow \rho(H(\theta_{\text{BBBS}}))$. Running optimization from other angles in \mathcal{M} (in addition to θ_{BBBS}) every iteration may also be advantageous, particularly if this can be done via parallel processing. Adding zero to the initial set \mathcal{M} avoids having to deal with any “wrap-around” level-set intervals due to the periodicity of $\rho(H(\theta))$, while θ_0 is just a reasonable initial guess for a global maximizer of (2.5).

generalized eigenvalue problem. Moreover, $H'(\theta)x_j$ would already be computed for $\rho'(H(\theta))$ and $H''(\theta)x_j = -H(\theta)x_j = -\lambda_j x_j$, so there is no other work of consequence to obtain $\rho''(H(\theta))$ via Theorem 3.4.

Pseudocode for our improved level-set algorithm is given in Algorithm 1. In Section 7, benchmarks verify that Algorithm 1 is much faster than Mengi and Overton’s method, as it often only needs a single eigenvalue computation with $R_\gamma - \lambda S$, while Mengi and Overton’s method requires several. Even when optimization is disabled, our BBBS-like iteration using (2.5) is still faster than Mengi and Overton’s method.

We now address some practical implementation concerns. Whether Newton’s or secant method should be used depends on how much cheaper it is to solve eigenvalue problems with $H(\theta)$ relative to with $R_\gamma - \lambda S$. For the sizes tested, Table 1 shows that 27–140 `eig`($H(\theta)$) computations can be done before the total cost exceeds that of a single call of `eig`(R_γ, S). Whether eigenvalues of $H(\theta)$ should be computed with `eig` or `eigs` is also addressed. For dense matrices, requesting more than one eigenvalue from `eigs` (which should be done, as the desired eigenvalue may not always be the first to converge) was often slower than `eig`. For sparse matrices, `eigs` was sometimes up to five times faster than `eig`, but this means forgoing $\rho''(H(\theta))$ and Newton’s method, and so these gains may be offset by more optimization iterations. Thus, using Newton’s method with `eig`($H(\theta)$) for Algorithm 1 seems most appropriate, while `eigs` may be preferred for Uhlig’s method, where only $\lambda_{\max}(H(\theta))$ is needed.

There are a couple of other important details for implementing Algorithm 1. At each iteration, the spectrum of $R_\gamma - \lambda S$ is computed using $\gamma := \gamma(1 + \tau_{\text{tol}})$, where $\tau_{\text{tol}} > 0$ is some relative termination tolerance. This helps to prevent computing eigenvalues of multiple instances of $R_\gamma - \lambda S$ once $\gamma \approx r(A)$, particularly since maximizers of (2.5) generally will not be found exactly. Furthermore, if $\gamma = r(A)$ does hold numerically, then $R_\gamma - \lambda S$ cannot have any unimodular eigenvalues for $\gamma := \gamma(1 + \tau_{\text{tol}})$, thus ensuring termination. Another issue that may arise is due to double (or higher multiplicity) eigenvalues of $R_\gamma - \lambda S$. Suppose that θ_{BBBS} is the argument of a double unimodular eigenvalue of $R_\gamma - \lambda S$, where $\gamma = \rho(H(\theta_{\text{BBBS}}))$ and θ_{BBBS} is a local minimizer of $\rho(H(\theta))$. If rounding errors prevent this double eigenvalue from being detected, the resulting level-set interval $[\theta_k, \theta_{k+1}]$ will contain θ_{BBBS} in its interior. If θ_{BBBS} also happens

Table 1: Running times normalized to $\text{eig}(H(\theta))$, i.e., the running time of a given operation divided by the corresponding running time of $\text{eig}(H(\theta))$ for random A matrices. For $H(\theta)$, eigenvectors were requested (as they are needed), while only eigenvalues were requested for $S^{-1}R_\gamma$ and $R_\gamma - \lambda S$. For numerical robustness, $R_\gamma - \lambda S$ should be used, preferably with a structure-preserving eigensolver, e.g., [BBMX02, BSV16], since S^{-1} may be ill-conditioned (S^{-1} exists if and only if A is invertible). For `eigs`, k is the number of eigenvalues requested, while 'LM' (largest modulus), 'LR' (largest real), and 'BE' (both ends) specifies which eigenvalues are desired.

		<code>eigs</code> ($H(\theta)$, k , 'LM')		<code>eigs</code> ($H(\theta)$, k , 'LR')		<code>eigs</code> ($H(\theta)$, k , 'BE')			<code>eig</code> (\cdot)	
	n	$k = 1$	$k = 6$	$k = 1$	$k = 6$	$k = 2$	$k = 4$	$k = 6$	$S^{-1}R_\gamma$	$R_\gamma - \lambda S$
Dense A	200	1.5	3.2	1.5	1.5	1.2	1.3	1.7	11.5	26.8
	400	0.8	1.3	0.6	1.1	1.2	1.1	1.2	14.9	63.5
	800	0.8	1.5	0.7	1.4	1.5	1.2	1.4	14.7	101.8
	1600	0.5	0.9	0.5	0.8	1.0	0.9	0.9	15.2	139.8
Sparse A	200	1.3	1.6	0.8	1.3	1.4	1.3	1.8	21.1	27.5
	400	0.4	0.6	0.3	0.5	0.5	0.5	0.5	12.8	45.7
	800	0.3	0.5	0.2	0.5	0.4	0.5	0.5	14.0	92.2
	1600	0.2	0.3	0.2	0.3	0.3	0.3	0.3	13.8	131.8

to be its midpoint (or near to it), then the algorithm may get stuck here, precisely because $\gamma = \rho(H(\theta_{\text{BBBS}}))$. Note that this issue can occur even in the standard BBBS iteration. As pointed out in [BLO03, p. 372–373] for the criss-cross algorithm for the pseudospectral abscissa, a robust fix is simple: split any level-set interval $[\theta_k, \theta_{k+1}]$ into $[\theta_k, \theta_{\text{BBBS}}]$ and $[\theta_{\text{BBBS}}, \theta_{k+1}]$ whenever $\theta_{\text{BBBS}} \approx 0.5(\theta_k + \theta_{k+1})$.

4 Analysis of Uhlig's method

We now establish two convergence results for Uhlig's method. For the special (and easier) case of disk matrices, we determine the exact number of supporting hyperplanes required by Uhlig's method in order to compute $r(A)$ to a desired accuracy and show that it blows up as more digits are requested. Subsequently, for general non-disk matrices A with $W(A)$ of any shape, we derive the exact Q-linear local rate of convergence for how quickly the cutting strategy proposed by Uhlig sufficiently approximates the boundary of $W(A)$ about an outermost point, which is necessary in order to estimate $r(A)$. We note now that our theory here also accurately reflects the overall cost of Uhlig's method in practice, all of which is clearly demonstrated by our experiments in Section 7.

4.1 Uhlig's method for disk matrices

For disk matrices, it is possible to completely describe the behavior of Uhlig's method to estimate $r(A)$, as is summarized in the following result showing that cutting-plane methods can be extremely expensive. Note that Uhlig's method begins with a rectangular approximation to $W(A)$, and for a disk matrix, this approximation is a square centered at the origin.

Theorem 4.1. *Suppose that $A \in \mathbb{C}^{n \times n}$ is a disk matrix with $r(A) > 0$ and that $W(A)$ is currently approximated by a regular polygon with $k \geq 3$ vertices, i.e., the approximation \mathcal{P}_k is given by k supporting hyperplanes specified by angles $\bar{\theta}_j = \frac{2\pi}{k}j$ for $j = 1, \dots, k$. Furthermore, let $\tau_{\text{tol}} \geq 0$ be a relative tolerance for the numerical radius estimate $r_{\text{ub}}(A, \mathcal{P}_k)$, i.e., $r_{\text{err}}(A, \mathcal{P}_k) \leq \tau_{\text{tol}}$ is desired, where $r_{\text{ub}}(A, \mathcal{P}_k)$ and $r_{\text{err}}(A, \mathcal{P}_k)$ are defined in (2.8). Then*

- (i) for any corner c of \mathcal{P}_k , the relative error $\frac{|c| - r(A)}{r(A)} = \sec\left(\frac{\pi}{k}\right) - 1$,
- (ii) $r_{\text{err}}(A, \mathcal{P}_k) = \sec\left(\frac{\pi}{k}\right) - 1$,

(iii) if $r_{\text{err}}(A, \mathcal{P}_k) \leq \tau_{\text{tol}}$, then $k \geq \left\lceil \frac{\pi}{\text{arcsec}(1+\tau_{\text{tol}})} \right\rceil$.

Moreover, if Uhlig's method is initialized with a regular polygon of k_0 vertices with $k_0 \geq 3$ and currently has \mathcal{P}_k as an approximation to $W(A)$, then

(iv) to obtain a lower error than $r_{\text{err}}(A, \mathcal{P}_k)$, Uhlig's method must refine \mathcal{P}_k into \mathcal{P}_{2k} , a regular polygon of $2k$ vertices, i.e., the number of vertices must be doubled,

(v) if $r_{\text{err}}(A, \mathcal{P}_k) \leq \tau_{\text{tol}}$, the number of doublings of vertices incurred from k_0 must be at least $d_{\text{min}} = \left\lceil \log_2 \left(\frac{\pi}{k_0 \text{arcsec}(1+\tau_{\text{tol}})} \right) \right\rceil$ and $k \geq k_0 \cdot 2^{d_{\text{min}}}$.

Proof. As $W(A)$ is a disk centered at the origin with radius $r(A)$ and \mathcal{P}_k is a regular polygon with $W(A)$ inscribed inside it, \mathcal{P}_k must also be centered at the origin, and so the moduli of all of its corners are identical. Thus, consider the corner c with $\text{Arg}(c) = \frac{\pi}{k}$ and the right triangle with hypotenuse defined by c and the origin and with the third point being $r(A)$ on the real axis. Then $|c|/r(A) = \sec(\frac{\pi}{k})$ and subtracting one from both sides yields (i) and (ii). As (iii) assumes that $\sec(\frac{\pi}{k}) - 1 \leq \tau_{\text{tol}}$, the claim is simply proven by a combination of rearranging terms and taking the inverse of the secant function. For (iv), since $r_{\text{err}}(A; \mathcal{P}_k)$ is defined as a maximum over the moduli of all the corners of \mathcal{P}_k , and by (i) their moduli are identical, every outermost corner of \mathcal{P}_k must be refined to lower the error; hence, k new supporting hyperplanes must be added. Due to the symmetry, Uhlig's cutting procedure simply amounts to bisecting the angles of adjacent supporting hyperplanes, and Uhlig's cutting procedure always selects an outermost corner to refine. Thus, a regular polygon with $2k$ vertices must be created after k more cuts. For (v), starting with a k_0 -vertex regular polygon means that d doublings of vertices results in an approximation to $W(A)$ with $k_0 \cdot 2^d$ vertices, and by (iv), the error is only lowered with each doubling of the number of vertices. Using (iii) with $k = k_0 \cdot 2^d$ and solving for d yields the minimum number of doublings required given by d_{min} above. \square

In Table 2, we apply Theorem 4.1 and report the minimum number of supporting hyperplanes needed to compute the numerical radius of disk matrices for different levels of accuracy. Clearly, the cost of Uhlig's method skyrockets as more accuracy is requested. As such, when computing the numerical radius of disk matrix to more than just a few digits, a level-set method, like Algorithm 1, is much faster.

Table 2: For any disk matrix A , the minimum number of supporting hyperplanes required to compute $r(A)$ to different accuracies is shown, where $\text{eps} \approx 2.22 \times 10^{-16}$.

Relative Tolerance	# of supporting hyperplanes needed		
	Minimum	Uhlig's method	
	$k_0 = 3$	$k_0 = 4$	
$\tau_{\text{tol}} = 1\text{e-}4$	223	384	256
$\tau_{\text{tol}} = 1\text{e-}8$	22 215	24 576	32 768
$\tau_{\text{tol}} = 1\text{e-}12$	2 221 343	3 145 728	4 194 304
$\tau_{\text{tol}} = \text{eps}$	149 078 414	201 326 592	268 435 456

4.2 Analysis for arbitrary field of values

We now assume that $W(A)$ takes on any possible shape, except a disk centered at the origin, and so $W(A)$ has at most n outermost points (see Section 2). We will use the concept of Q-linear and Q-superlinear convergence, where “Q” stands for “quotient”; see [NW99, p. 619] for more details.

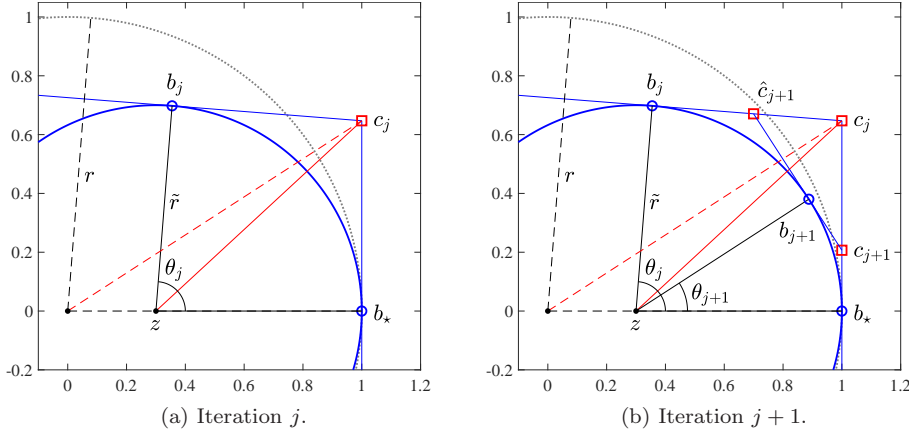


Figure 1: Depiction of Uhlig's method where $W(A)$ is a disk of radius $\tilde{r} = 0.7$ centered at $z = 0.3$, and so $r = r(A) = 1$ is attained at the point b_* $\in \partial W(A)$. The dotted circle is the circle of radius $r(A) = 1$ centered at the origin.

Key Remark 4.2. *In order for $r_{\text{err}}(A, \mathcal{P}_k)$ to be small, sections of $\partial W(A)$ close to the circle with radius $r(A)$ centered at the origin must be well approximated, while regions of $\partial W(A)$ farther away from this circle need only be crudely approximated. Thus, whether Uhlig's method is fast or slow only hinges upon its cost to sufficiently well approximate $\partial W(A)$ about the outermost points in $W(A)$ that attain $r(A)$.*

Key Remark 4.3. *It is unnecessary to consider the exact boundary of $W(A)$ to determine the efficiency of a cutting-plane method. Per Key Remark 2.4, it suffices to study how quickly the cutting-plane procedure can approximate the relevant arcs of the osculating circles of $\partial W(A)$ at the outermost points of $W(A)$, which amounts to a convergence analysis where the third-order terms are dropped.*

While curvature of $\partial W(A)$ will play a role in our analysis, the salient property to consider is how close $\partial W(A)$ resembles the field of values boundary of a disk matrix in neighborhoods about outermost points in $W(A)$. We can concisely characterize this property by introducing what we call *normalized curvature* at outermost points.

Definition 4.4. *Let b_* be an outermost point of $W(A)$, and per Definition 2.3, let $\tilde{r} \geq 0$ be the radius of the osculating circle of $\partial W(A)$ at b_* . The normalized curvature μ of $\partial W(A)$ at b_* is*

$$\mu := \frac{\tilde{r}}{r(A)} \in [0, 1].$$

Thus, $\mu = 0$ corresponds to b_ being a corner of $\partial W(A)$, while in a neighborhood about b_* , $\partial W(A)$ becomes more and more like an arc of the circle with radius $r(A)$ centered at the origin as $\mu \rightarrow 1$, with exact agreement for $\mu = 1$.*

Example 4.5 (See Fig. 1 for a visual description). *For $n \geq 2$, consider $A = zI + \tilde{r}K_n$, where $K_n \in \mathbb{C}^{n \times n}$ is any disk matrix with $r(K_n) = 1$, e.g., (2.9), $\tilde{r} > 0$, and $z \geq 0$. Thus, $W(A)$ is a disk with radius \tilde{r} centered at z on the real axis, where $r(A)$ is attained at $b_* = z + \tilde{r} \in \partial W(A)$. Clearly, the radius of the osculating circle of $\partial W(A)$ at b_* is also \tilde{r} , and so the normalized curvature of $\partial W(A)$ at b_* is $\mu = \frac{\tilde{r}}{r}$, where $r := r(A)$, a shorthand we will often use in Section 4 and Section 5. Suppose \mathcal{P}_j contains the supporting hyperplane for $\overline{\theta}_* = -\text{Arg}(b_*) = 0$ and that $b_j \in \partial W(A)$ is the next tangential boundary point in \mathcal{P}_j , in the counter-clockwise direction with respect to b_* . Let c_j be the corner of \mathcal{P}_j between b_j and b_* and suppose c_j is cut*

next. This results in the new tangential boundary point b_{j+1} and two new corners, \hat{c}_{j+1} and c_{j+1} , which we respectively refer to as counter-clockwise (CCW) and clockwise (CW) corners due to their orientation with respect to b_{j+1} . Note that Uhlig's method cuts c_j by adding the supporting hyperplane for $\bar{\theta}_j = -\text{Arg}(c_j)$ to \mathcal{P}_j . Finally, let $\{c_k\}$ denote the sequence of corners produced by any cutting procedure, Uhlig's or otherwise, if it is only applied to the CW corners, i.e., $\{c_k\} = c_j, c_{j+1}, \dots$, all of which lie on the tangent line $L_{\bar{\theta}_*}$ passing through b_* . For all $k \geq j$, we have that $r(A) < |c_k|$ for any CW corner c_k , while any CCW corner \hat{c}_k such that $|\hat{c}_k| \leq r(A)$ does not need to be refined/cut.

Assumption 4.6. Let $b_* \in W(A)$ be such that $|b_*| = r(A) > 0$, \mathcal{P}_j be the current approximation to $W(A)$ via supporting hyperplanes, i.e., (2.7), and let $b_j \neq b_*$ be the first tangential boundary point of $W(A)$ in \mathcal{P}_j in the counter-clockwise direction with respect to b_* . We assume that

- (i) the normalized curvature of $\partial W(A)$ at b_* is $\mu \in (0, 1]$,
- (ii) $P_{\bar{\theta}_*} \subset \mathcal{P}_j$, where $\bar{\theta}_* = -\text{Arg}(b_*)$, i.e., b_* is a tangential boundary point in \mathcal{P}_j ,
- (iii) b_j is sufficiently close to b_* such that Key Remark 4.3 applies.

Without loss of generality, we can also assume that $\text{Arg}(b_*) = 0$, as A can be rotated, and so the supporting line $L_{\bar{\theta}_*}$ associated with $P_{\bar{\theta}_*}$ is vertical, passing through b_* on the real axis.

Key Remark 4.7. Under Assumption 4.6, analyzing the efficiency of any cutting-plane method to sufficiently well approximate any shaped $\partial W(A)$ about any outermost point of $W(A)$ simplifies to analyzing Example 4.5, and in particular, $\{c_k\}$.

Some comments on Assumption 4.6 are in order. While we have assumed that the outermost point b_* is not a corner, i.e., $\mu > 0$, this is not a limitation; our analysis gives an exact Q-linear rate of convergence for any $\mu \in (0, 1]$, and as $\mu \rightarrow 0$, it becomes Q-superlinear. The assumption that the outermost point b_* is known to the algorithm, i.e., it is a tangential boundary point in \mathcal{P}_j , is actually very mild. Although Uhlig's method may sometimes only obtain such points in the limit as it converges, they can actually be cheaply added to \mathcal{P}_j via a simple modification, namely, by also incorporating the fast local optimization techniques discussed in Section 3. For non-disk matrices, each of the at most n outermost points in $W(A)$ is “bracketed” on $\partial W(A)$ by two tangential boundary points in \mathcal{P}_j , and these brackets improve as \mathcal{P}_j more accurately approximates $W(A)$ and/or other outermost points of $W(A)$ are found. Once \mathcal{P}_j is no longer a crude approximation, the arguments of these bracketing tangential boundary points can be used to initialize optimization to find global maximizers of $h(\theta)$, and thus, globally outermost points of $W(A)$.

Lemma 4.8. If the sequence of corners $\{c_k\}$ described in Example 4.5 is produced by Uhlig's cutting procedure, so $\theta_k := \text{Arg}(b_k - z)$ and $\bar{\theta}_k = -\theta_k$ is the angle associated with the supporting plane for b_k , then, for all $k \geq j$,

$$\theta_{k+1} = \text{Arg}(b_{k+1} - z) = \arctan\left(\mu \tan \frac{1}{2}\theta_k\right). \quad (4.1)$$

Proof. The result holds via the following geometric argument. First note that

$$\tilde{r} \tan \frac{1}{2}\theta_k = |c_k - b_*| \quad \text{and} \quad \text{Arg}(c_k) = \arctan(r^{-1}|c_k - b_*|).$$

Substituting the left equation into the right one yields $\text{Arg}(c_k) = \arctan\left(\mu \tan \frac{1}{2}\theta_k\right)$. Then (4.1) follows by additionally noting that $\text{Arg}(c_k) = \text{Arg}(b_{k+1} - z)$ also holds. \square

Theorem 4.9. Under Assumption 4.6, the sequence $\{\theta_k\}$ produced by Uhlig's cutting procedure and described by (4.1) converges to zero Q-linearly with rate $\frac{1}{2}\mu$.

Proof. First note that $\lim_{k \rightarrow \infty} \theta_k = \theta_\star = 0$ and $\theta_k > 0$ for all $k \geq j$. Then

$$\lim_{k \rightarrow \infty} \frac{|\theta_{k+1} - \theta_\star|}{|\theta_k - \theta_\star|} = \lim_{k \rightarrow \infty} \frac{\theta_{k+1}}{\theta_k} = \lim_{k \rightarrow \infty} \frac{\arctan(\mu \tan \frac{1}{2}\theta_k)}{\theta_k}.$$

Since the numerator and denominator both go to zero as $k \rightarrow \infty$, the result follows by considering the continuous version of the limit:

$$\lim_{\theta \rightarrow 0} \frac{\arctan(\mu \tan \frac{1}{2}\theta)}{\theta} = \lim_{\theta \rightarrow 0} \frac{\mu \tan \frac{1}{2}\theta}{\theta} = \lim_{\theta \rightarrow 0} \frac{\frac{1}{2}\mu\theta}{\theta} = \frac{1}{2}\mu,$$

where the first and second equalities are obtained, respectively, using small-angle approximations $\arctan x \approx x$ and $\tan x \approx x$ for $x \approx 0$. \square

While Theorem 4.9 tells us how quickly $\{\theta_k\}$ will converge, we really want to estimate how quickly $r_{\text{err}}(A, \mathcal{P}_j)$ becomes sufficiently small. For that, we instead must consider how fast the moduli of the corresponding outermost corners c_k converge.

Theorem 4.10. *Under Assumption 4.6 and considering $\{\theta_k\}$ from Theorem 4.9, the associated sequence $\{|c_k|\}$ converges to $r(A)$ Q -linearly with rate $\frac{1}{4}\mu^2$.*

Proof. Recalling that $r = r(A)$, first note that

$$\cos \theta_{k+1} = \frac{r}{|c_k|} \quad \text{and so} \quad |c_k| = r \sec \theta_{k+1} > r$$

for all $k \geq j$. Thus, we consider the limit

$$\lim_{k \rightarrow \infty} \frac{|c_{k+1}| - r}{|c_k| - r} = \lim_{k \rightarrow \infty} \frac{r \sec \theta_{k+2} - r}{r \sec \theta_{k+1} - r} = \lim_{k \rightarrow \infty} \frac{\sec \theta_{k+1} - 1}{\sec \theta_k - 1},$$

which when substituting in $\theta_{k+1} = \arctan(\mu \tan \frac{1}{2}\theta_k)$ becomes

$$\lim_{k \rightarrow \infty} \frac{\sec(\arctan(\mu \tan \frac{1}{2}\theta_k)) - 1}{\sec \theta_k - 1}.$$

Since the numerator and denominator both go to zero as $k \rightarrow \infty$, we consider the continuous version of the limit, i.e.,

$$\lim_{\theta \rightarrow 0} \frac{\sec(\arctan(\mu \tan \frac{1}{2}\theta)) - 1}{\sec \theta - 1} = \lim_{\theta \rightarrow 0} \frac{\sec(\mu \tan \frac{1}{2}\theta) - 1}{\sec \theta - 1} = \lim_{\theta \rightarrow 0} \frac{\sec(\frac{1}{2}\mu\theta) - 1}{\sec \theta - 1},$$

again using the small-angle approximations for \arctan and \tan . As this is an indeterminant form, we will apply L'Hôpital's Rule. However, it will be convenient to first multiply by the following identity to get rid of the $\sec \theta$ in the denominator:

$$\lim_{\theta \rightarrow 0} \frac{\cos \theta}{\cos \theta} \cdot \frac{\sec(\frac{1}{2}\mu\theta) - 1}{\sec \theta - 1} = \lim_{\theta \rightarrow 0} \frac{\cos \theta (\sec(\frac{1}{2}\mu\theta) - 1)}{1 - \cos \theta} = \lim_{\theta \rightarrow 0} \frac{f_1(\theta)}{f_2(\theta)}.$$

For $f_2(\theta)$, $f'_2(\theta) = \sin \theta$, while for $f_1(\theta)$, we have

$$\begin{aligned} f'_1(\theta) &= -\sin \theta (\sec(\frac{1}{2}\mu\theta) - 1) + \frac{1}{2}\mu \cos \theta \cdot \sec(\frac{1}{2}\mu\theta) \cdot \tan(\frac{1}{2}\mu\theta) \\ &= -\sin \theta (\sec(\frac{1}{2}\mu\theta) - 1) + \frac{1}{2}\mu \cos \theta \cdot \frac{\sin(\frac{1}{2}\mu\theta)}{\cos^2(\frac{1}{2}\mu\theta)}, \end{aligned}$$

where the second equality uses that $\sec x = \frac{1}{\cos x}$ and $\tan x = \frac{\sin x}{\cos x}$. As $f'_1(0) = 0$ and $f'_2(0) = 0$, we still have an indeterminate form and so will again apply L'Hôpital's Rule. For the denominator, we have $f''_2(\theta) = \cos \theta$ and so $f''_2(0) = 1$. For the numerator, it will be convenient to write $f'_1(\theta) = -g_1(\theta) + \frac{1}{2}\mu g_2(\theta)$, where

$$g_1(\theta) = \sin \theta (\sec(\frac{1}{2}\mu\theta) - 1) \quad \text{and} \quad g_2(\theta) = \cos \theta \cdot \frac{\sin(\frac{1}{2}\mu\theta)}{\cos^2(\frac{1}{2}\mu\theta)},$$

and differentiate the parts separately. For $g_1(\theta)$, we have that

$$g'_1(\theta) = \cos \theta (\sec(\frac{1}{2}\mu\theta) - 1) + \frac{1}{2}\mu \sin \theta \cdot \sec(\frac{1}{2}\mu\theta) \cdot \tan(\frac{1}{2}\mu\theta),$$

and so $g'_1(0) = 0$. For $g_2(\theta)$, we have that

$$g'_2(\theta) = -\sin \theta \cdot \frac{\sin(\frac{1}{2}\mu\theta)}{\cos^2(\frac{1}{2}\mu\theta)} + \cos \theta \cdot \frac{\frac{1}{2}\mu (\cos^3(\frac{1}{2}\mu\theta) + 2\sin^2(\frac{1}{2}\mu\theta) \cdot \cos(\frac{1}{2}\mu\theta))}{\cos^4(\frac{1}{2}\mu\theta)},$$

and so $g'_2(0) = \frac{1}{2}\mu$. Thus, $f''_1(0) = -g'_1(0) + \frac{1}{2}\mu g'_2(0) = \frac{1}{4}\mu^2$, proving the claim. \square

Together, Theorems 4.9 and 4.10 give the exact Q-linear rate of convergence of Uhlig's cutting procedure and show that it is actually Q-superlinear at outermost points that are corners ($\mu = 0$). Theorem 4.10 also allows us to estimate the cost of approximating $\partial W(A)$ about outermost points. Using Example 4.5, we can determine how many iterations will be needed until it is no longer necessary to refine corner c_k , i.e., the value of k such that $|c_k| \leq r(A) \cdot (1 + \tau_{\text{tol}})$. For simplicity, it will be more convenient to assume that c_j is c_0 , with $|c_0| = s_0 r(A)$ for some scalar $s_0 > (1 + \tau_{\text{tol}})$. Using the Q-linear rate given by Theorem 4.10, we have that

$$|c_k| - r(A) \leq (|c_0| - r(A)) \cdot (\frac{1}{4}\mu^2)^k,$$

and so if

$$r(A) + (|c_0| - r(A)) \cdot (\frac{1}{4}\mu^2)^k \leq r(A) \cdot (1 + \tau_{\text{tol}}),$$

then it follows that $|c_k| \leq r(A) \cdot (1 + \tau_{\text{tol}})$, i.e., it does not need to be refined further. By first dividing the above equation by $r(A)$ and doing some simple manipulations, we have that $|c_k|$ is indeed sufficiently close to $r(A)$ if

$$k \geq \frac{\log(\tau_{\text{tol}}) - \log(s_0 - 1)}{\log(\frac{1}{4}\mu^2)}. \quad (4.2)$$

Using Example 4.5, $s_0 = 100$, and $\tau_{\text{tol}} = 1\text{e-}14$, only $k \approx 27, 14, 7$, and 4 iterations are needed, respectively, for $\mu = 1, 0.5, 0.1$, and 0.01 . While this is linear convergence, it is rather fast linear convergence. Of course, if $W(A)$ has more than one outermost point, the total cost of a cutting-plane method increases commensurately, since $\partial W(A)$ must be well approximated about all of these outermost points. For disk matrices, all boundary points are outermost, and so the cost blows up, per Theorem 4.1.

5 An improved cutting-plane algorithm

In Algorithm 2, we give pseudocode for our second improved iteration, which addresses some inefficiencies in Uhlig's method. The main two components of the algorithm are as follows. First, by also leveraging local optimization, as we have done for Algorithm 1, we can quickly locate outermost points in $W(A)$. Second, given a boundary point known to be locally outermost, we can invoke a new cutting procedure that reduces the total number of cuts needed to compute $r(A)$ to the desired level of accuracy. When this new cut cannot be invoked, we will fall back to Uhlig's cutting procedure. In the next three subsections, we describe our new cutting strategy, derive its Q-linear rate of convergence, and show how these cuts can be sufficiently well estimated so that our theoretical convergence rate result is indeed realized in practice.

Algorithm 2 An Improved Cutting-Plane Algorithm

Input: $A \in \mathbb{C}^{n \times n}$ and tolerance $\tau_{\text{tol}} > 0$.

Output: γ such that $|\gamma - r(A)| \leq \tau_{\text{tol}} \cdot r(A)$.

```
1:  $\theta_0 \leftarrow \text{Arg}(\lambda)$  where  $\lambda \in \Lambda(A)$  attains  $\rho(A)$  // 0 if  $\lambda = 0$ 
2:  $\mathcal{P}_0 \leftarrow$  the supporting hyperplanes given by angles  $[0, 0.5\pi, \pi, 1.5] - \theta_0$ 
3: for  $k = 0, 1, 2, \dots$  and while  $|r_{\text{ub}}(A; \mathcal{P}_{k+1}) - \gamma| > \gamma \cdot \tau_{\text{tol}}$  do
4:    $\gamma \leftarrow \max |b|$  over all tangential boundary points  $b \in \mathcal{P}_k$ 
5:    $\bar{\theta} \leftarrow$  angle of the supporting hyperplane associated with  $\arg \max |b|$ 
6:   if  $\rho(H(\bar{\theta})) \geq \gamma$  and  $\bar{\theta}$  is not a stationary point of  $\rho(H(\theta))$  then
7:      $\gamma \leftarrow$  maximization of  $\rho(H(\theta))$  via local optimization initialized at  $\bar{\theta}$ 
8:      $\mathcal{P}_k \leftarrow \mathcal{P}_k \cap P_{\bar{\theta}_1} \cap \dots \cap P_{\bar{\theta}_q}$  for all angles encountered during optimization
9:   end if
10:   $c \leftarrow$  outermost corner of  $\mathcal{P}_k$ 
11:  if the optimal cut can be applied to  $c$  per Section 5.3 then
12:     $\mathcal{P}_{k+1} \leftarrow \mathcal{P}_k \cap P_{\bar{\theta}}$  for angle  $\bar{\theta}$  given by (5.12)
13:  else
14:     $\mathcal{P}_{k+1} \leftarrow \mathcal{P}_k \cap P_{\bar{\theta}}$  for angle  $\bar{\theta} = -\text{Arg}(c)$  // Uhlig's cut
15:  end if
16: end for
```

NOTE: For simplicity, we forgo describing pseudocode to exploit symmetry of $W(A)$ and assume that there are no ties for the max in line 5. If there are ties, one could eliminate those that do not satisfy the conditional in line 6 and attempt optimization from the rest. Note that the rotation of the initial rectangular bounding box \mathcal{P}_0 for $W(A)$ is specified by θ_0 .

5.1 An improved optimal-cut strategy

Again consider Example 4.5. In Fig. 1b, Uhlig's cut of corner c_j between b_j (with $|b_j| < r$) and b_* produces two new corners \hat{c}_{j+1} and c_{j+1} , but since $|\hat{c}_{j+1}| < r$ and $|c_{j+1}| > r$, it is only necessary to subsequently refine c_{j+1} . However, in Fig. 2a we show another scenario where both of the two new corners produced by Uhlig's cut will require subsequent cutting as well. While Theorems 4.9 and 4.10 indicate the number of iterations Uhlig's method will need to sufficiently refine the sequence $\{c_k\}$, they do not take into account that the CCW corners that are generated may also need to be cut. Thus, the total number of eigenvalue computations with $H(\theta)$ can be higher than what is suggested by these two theorems. However, comparing Figs. 1b and 2a immediately suggests a better strategy, namely, to make the largest reduction in the angle θ_j (shown in these figures) such that the CCW corner \hat{c}_{j+1} (between b_j and c_j on the tangent line for b_j) does not need to be subsequently refined, i.e., such that $|\hat{c}_{j+1}| = r$. In Fig. 2a, this ideal corner is labeled d_j , while the corresponding optimal cut for this same example is shown in Fig. 2b, where d_j coincides with \hat{c}_{j+1} , and so the latter is not labeled.

5.2 Convergence analysis of the optimal cut

Per Key Remark 4.7, without loss of generality, it suffices to study Example 4.5 under Assumption 4.6 to determine the convergence rate of the sequence of angles $\{\theta_k\}$ produced by the optimal-cut strategy. For now, we assume these optimal cuts can be computed for general $\partial W(A)$, which we show how to do later. We begin by deriving the exact recursion formula for the sequence of angles associated with optimal cuts for Example 4.5.

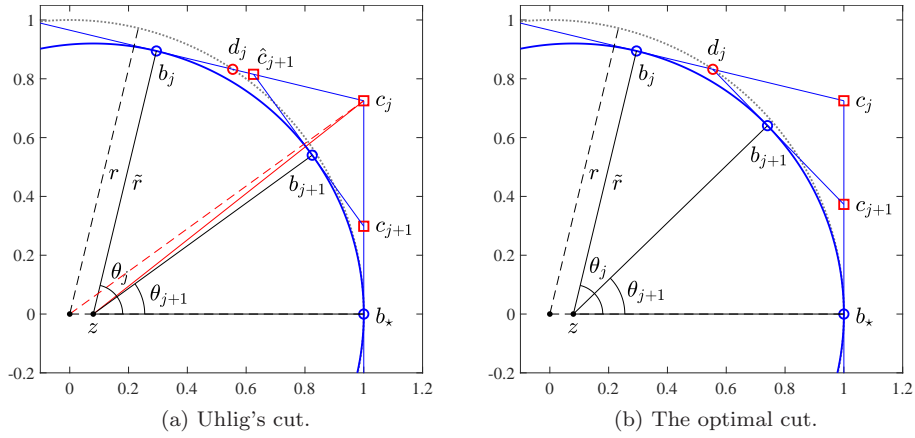


Figure 2: Depictions of corner c_j between tangential boundary points b_j and b_* being cut by Uhlig's procedure (left) and the optimal cut (right), where the latter always makes the largest possible reduction in θ_j such that only corner c_{j+1} must be refined.

Lemma 5.1. For Example 4.5 with $\mu \in (0, 1)$, consider corner c_j between tangential boundary points b_j and b_* with $|b_j| < |b_*| = r$, $\theta_j = \text{Arg}(b_j - z) \in (0, \pi)$, and $\text{Arg}(b_*) = 0$. The point d_j on the tangent line for b_j , closest to c_j , and $|d_j| = r$, is

$$d_j = b_j - it_j e^{i\theta_j}, \quad (5.1)$$

where $b_j = z + \tilde{r}e^{i\theta_j}$ and

$$t_j = -z \sin \theta_j + \sqrt{z^2 \sin^2 \theta_j - 2z\tilde{r}(\cos \theta_j - 1)} > 0. \quad (5.2)$$

Proof. Since $\theta_j \in (0, \pi)$, clearly (5.1) must hold for some $t_j > 0$. To obtain (5.2), we use the fact that $|d_j|^2 = r^2$ and solve for t_j using (5.1). Setting $u = e^{i\theta_j}$, we have

$$0 = |d_j|^2 - r^2 = (b_j - \mathbf{i}t_j u)(\bar{b}_j + \mathbf{i}t_j \bar{u}) - r^2 = t_j^2 + \mathbf{i}(b_j \bar{u} - \bar{b}_j u)t_j + |b_j|^2 - r^2.$$

which by substituting in the following two equivalences

$$b_j \bar{u} - \bar{b}_j u = (z + \tilde{r}u)\bar{u} - (z + \tilde{r}\bar{u})u = z(\bar{u} - u) = -i2z \sin \theta_j,$$

$$|b_j|^2 = z^2 + \tilde{r}^2 + z\tilde{r}(u + \bar{u}) = z^2 + \tilde{r}^2 + 2z\tilde{r} \cos \theta_j,$$

yields

$$0 = t_j^2 + (2z \sin \theta_j) t_j + (z^2 + \tilde{r}^2 - r^2 + 2z\tilde{r} \cos \theta_j).$$

By substituting in $r^2 = (z + \tilde{r})^2 = z^2 + \tilde{r}^2 + 2z\tilde{r}$, this simplifies further to

$$0 = t_j^2 + (2z \sin \theta_j) t_j + 2z \tilde{r} (\cos \theta_j - 1).$$

Thus, by the quadratic formula, we obtain (5.2).

Lemma 5.2. For Example 4.5 with $\mu \in (0, 1)$, given tangential boundary points b_j and b_* with $|b_j| < |b_*| = r$, $\theta_j = \text{Arg}(b_j - z) \in (0, \frac{\pi}{2})$, and $\text{Arg}(b_*) = 0$, the optimal cut for corner c_j produces angle

$$\theta_{j+1} = \text{Arg}(b_{j+1} - z) = -\theta_j + 2 \arctan \left(\frac{\tilde{r} \sin \theta_j - t_j \cos \theta_j}{\tilde{r} \cos \theta_j + t_j \sin \theta_j} \right), \quad (5.3)$$

where $t_j > 0$ and is defined by (5.2).

Proof. Let $\hat{\theta} = \theta_j - \text{Arg}(d_j - z)$. Then it follows that

$$\theta_{j+1} = \theta_j - 2\hat{\theta} = -\theta_j + 2 \text{Arg}(d_j - z) = -\theta_j + 2 \arctan \left(\frac{\text{Im}(d_j - z)}{\text{Re}(d_j - z)} \right),$$

where the last equality follows because $\text{Re}(d_j - z) > 0$, as $\text{Re} b_j > z$. Using (5.1) and substituting in $b_j = z + \tilde{r}e^{i\theta_j}$, we have that

$$d_j - z = \tilde{r}e^{i\theta_j} - it_j e^{i\theta_j} \implies \begin{aligned} \text{Re}(d_j - z) &= \tilde{r} \cos \theta_j + t_j \sin \theta_j, \\ \text{Im}(d_j - z) &= \tilde{r} \sin \theta_j - t_j \cos \theta_j, \end{aligned}$$

where $t_j > 0$ is given by (5.2). Substituting these inside the arctan in the equation above completes the proof. \square

Before determining how fast $\{\theta_k\}$ converges, we show that $\theta_k \rightarrow 0$ indeed holds.

Lemma 5.3. *Given the assumptions of Lemma 5.2, the recursion (5.3) for optimal cuts is a sequence of angles $\{\theta_k\}$ converging to zero.*

Proof. By construction, $\{\theta_k\}$ is monotone, i.e., $\theta_{k+1} < \theta_k$ for all k , and bounded below by zero, and so $\{\theta_k\}$ converges to some limit l . Per (5.2), the t_j values appearing in (5.3) depend on θ_j , so we define the analogous continuous function

$$t(\theta) = -z \sin \theta + \sqrt{z^2 \sin^2 \theta - 2z\tilde{r}(\cos \theta - 1)}. \quad (5.4)$$

Now by way of contradiction, assume that $l > 0$ and so $0 < l < \theta_j < \frac{\pi}{2}$. Thus,

$$\lim_{k \rightarrow \infty} \theta_{k+1} = l = -l + 2 \arctan \left(\frac{\tilde{r} \sin l - t(l) \cos l}{\tilde{r} \cos l + t(l) \sin l} \right) \Rightarrow \tan l = \frac{\tilde{r} \sin l - t(l) \cos l}{\tilde{r} \cos l + t(l) \sin l}.$$

Multiplying both sides by $\tilde{r} \cos l + t(l) \sin l$ yields

$$\tilde{r} \sin l + t(l) \frac{\sin^2 l}{\cos l} = \tilde{r} \sin l - t(l) \cos l \Rightarrow t(l) \frac{\sin^2 l + \cos^2 l}{\cos l} = 0,$$

which implies $t(l) = 0$, which contradicts the statement in (5.2) that the t_j values are always positive. Thus, $l = 0$. \square

We now have the necessary pieces to derive the exact rate of convergence of the angles produced by optimal cuts about an outermost point of any shaped $W(A)$.

Theorem 5.4. *Given Assumption 4.6 and the additional assumptions given in Lemma 5.2, the sequence $\{\theta_k\}$ produced by optimal cuts and described by (5.3) converges to zero Q -linearly with rate $\frac{2(1-\sqrt{1-\mu})}{\mu} - 1$.*

Proof. By Lemmas 5.2 and 5.3, (5.3) holds, $\theta_k \rightarrow 0$, and $\theta_k \geq 0$ for all k , so

$$\lim_{k \rightarrow \infty} \frac{|\theta_{k+1} - \theta_*|}{|\theta_k - \theta_*|} = \lim_{k \rightarrow \infty} \frac{\theta_{k+1}}{\theta_k} = \lim_{k \rightarrow \infty} \frac{-\theta_k + 2 \arctan \left(\frac{\tilde{r} \sin \theta_k - t_k \cos \theta_k}{\tilde{r} \cos \theta_k + t_k \sin \theta_k} \right)}{\theta_k}.$$

Using the continuous version of t_k given in (5.4), we instead consider the entire limit in continuous form:

$$\lim_{\theta \rightarrow 0} \frac{-\theta + 2 \arctan \left(\frac{\tilde{r} \sin \theta - t(\theta) \cos \theta}{\tilde{r} \cos \theta + t(\theta) \sin \theta} \right)}{\theta} = -1 + \lim_{\theta \rightarrow 0} \frac{2}{\theta} \cdot \frac{\tilde{r} \theta - t(\theta) \cos \theta}{\tilde{r} \cos \theta + t(\theta) \theta}, \quad (5.5)$$

where the equality holds by using the small-angle approximations $\arctan x \approx x$ (as the ratio inside the arctan above goes to zero as $\theta \rightarrow 0$) and $\sin x \approx x$. Again using $\sin x \approx x$ as well as the small-angle approximation $1 - \cos x \approx \frac{x^2}{2}$, we also have the small-angle approximation

$$t(\theta) \approx -z\theta + \sqrt{z^2\theta^2 - 2z\tilde{r}\left(\frac{-\theta^2}{2}\right)} = -\theta\left(z - \theta\sqrt{z^2 + z\tilde{r}}\right) = -\theta\left(z - \sqrt{zr}\right), \quad (5.6)$$

where the last equality holds by substituting in $\tilde{r} = r - z$. Via substituting in (5.6), the limit on the right-hand side of (5.5) is

$$\lim_{\theta \rightarrow 0} \frac{2}{\theta} \cdot \frac{\tilde{r}\theta + \theta(z - \sqrt{zr})\cos\theta}{\tilde{r}\cos\theta - \theta(z - \sqrt{zr})\theta} = \lim_{\theta \rightarrow 0} \frac{2(\tilde{r} + (z - \sqrt{zr})\cos\theta)}{\tilde{r}\cos\theta - \theta^2(z - \sqrt{zr})} = \frac{2(\tilde{r} + z - \sqrt{zr})}{\tilde{r}}.$$

Recalling that $\tilde{r} = \mu r$ and that $z = r - \tilde{r} = r - \mu r$, by substitutions we can rewrite the ratio above as

$$\frac{2\left(\mu r + (r - \mu r) - \sqrt{(r - \mu r)r}\right)}{\mu r} = \frac{2(r - r\sqrt{1 - \mu})}{\mu r} = \frac{2(1 - \sqrt{1 - \mu})}{\mu}.$$

Subtracting one from the value above completes the proof. \square

As we will show momentarily, the optimal cut is more efficient in terms of overall cost than Uhlig's cutting procedure. Thus, there is no need to derive an analogue of Theorem 4.10 that describes the convergence rate of the moduli of corners c_k produced by the optimal-cut strategy.

5.3 Computing the optimal cut

While we have used Example 4.5 to analyze the convergence rate of the optimal-cut strategy at an outermost point of $W(A)$, the optimal cut can also be used before the region of $\partial W(A)$ at an outermost point is well modeled by the osculating circle at that point. In fact, the optimal cut can also be invoked at a locally outermost point, provided that it is currently the outermost tangential boundary point in \mathcal{P}_j . Given such a locally or globally outermost point b_* with $|b_*| = \gamma \leq r$ and the next tangential boundary point b_j in the counter-clockwise direction (again, see Example 4.5 for a visual depiction), we will model the region of $\partial W(A)$ between b_* and b_j by fitting a quadratic that interpolates $\partial W(A)$ at b_* and b_j , while also being tangent at b_* . If this quadratic model appears to be a good fit, then we can use it to estimate d_j , and thus, the optimal cut. Clearly this quadratic model must be a good fit if b_j is sufficiently close to b_* , but it also allows modeling $\partial W(A)$ when b_j is farther away and the shape of $\partial W(A)$ is more parabolic. Once a globally outermost point has been found, the optimal cut will only be applied at globally outermost points of $W(A)$. While this interpolation-based computation of the optimal cut is not exact, we stress now that it is sufficiently accurate to realize the convergence rate of Theorem 5.4 in practice, which we demonstrate in Section 7.

Without loss of generality, we again assume that $\text{Arg}(b_*) = 0$ and $\text{Arg}(b_j) \in (0, \pi)$, and so we will fit a sideways quadratic (opening up to the left in the complex plane)

$$q(y) = q_2 y^2 + q_1 y + q_0,$$

to $\partial W(A)$ by passing through b_j and b_* . This leaves one remaining degree of freedom to determine $q(y)$ uniquely, and since b_* is a locally/globally outermost point of $W(A)$, we also specify that $q(y)$ should be tangent to $W(A)$ at b_* . Obviously, $q(y)$ may only be a good fit of $\partial W(A)$ if the tangent line for b_j is decreasing from left to right in the complex plane, i.e., $\bar{\theta}_j \in (-\frac{\pi}{2}, 0)$. Let angle $\bar{\theta}_{\text{Opt}} \in (\bar{\theta}_j, 0)$ denote the angle of the supporting hyperplane associated with the optimal cut, i.e., the one that passes through d_j and provides the new tangential boundary point b_{j+1} between b_j and b_* . We now show how to estimate $\bar{\theta}_{\text{Opt}}$.

By our interpolation criteria given above, q_0 , q_1 , and q_2 are determined by

$$q(0) = \gamma, \quad q(\operatorname{Im} b_j) = \operatorname{Re} b_j, \quad \text{and} \quad q'(0) = 0. \quad (5.7)$$

Solving these equations yields

$$q_2 = \frac{\operatorname{Re} b_j - \gamma}{(\operatorname{Im} b_j)^2}, \quad q_1 = 0, \quad \text{and} \quad q_0 = \gamma. \quad (5.8)$$

We can assess whether $q(y)$ is a good fit for $\partial W(A)$ about b_* by checking how close $q(y)$ is to being tangent to $\partial W(A)$ at b_j , i.e., $q(y)$ is a good fit if

$$q'(\operatorname{Im} b_j) \approx \tan \bar{\theta}_j. \quad (5.9)$$

If these two values are not sufficiently close, then we will consider $q(y)$ a poor local approximation of $\partial W(A)$ at b_j (and b_*) and will not attempt do an optimal cut; in this case, we just use Uhlig's cutting procedure instead. Otherwise, we can assume that $q(y)$ does accurately reflect the region of $\partial W(A)$ between b_j and b_* , and so we estimate $\bar{\theta}_{\text{Opt}}$ as follows. Given our good model $q(y)$, we need to determine the line

$$l(y) = l_1 y + l_0$$

such that $l(y)$ passes through d_j for $y = \operatorname{Im} d_j$ and is tangent to the quadratic $q(y)$ for some $\tilde{y} \in (0, \operatorname{Im} d_j)$. Thus, we solve the following set of equations in order to determine l_0 , l_1 and \tilde{y} :

$$\operatorname{Re} d_j = l(\operatorname{Im} d_j) \iff \operatorname{Re} d_j = l_1 \operatorname{Im} d_j + l_0, \quad (5.10a)$$

$$q(\tilde{y}) = l(\tilde{y}) \iff q_2 \tilde{y}^2 + q_0 = l_1 \tilde{y} + l_0, \quad (5.10b)$$

$$q'(\tilde{y}) = l'(\tilde{y}) \iff 2q_2 \tilde{y} = l_1. \quad (5.10c)$$

Solving these equations yields

$$\tilde{y} = \operatorname{Im} d_j - \sqrt{(\operatorname{Im} d_j)^2 + \frac{q_0 - \operatorname{Re} d_j}{q_2}}, \quad l_0 = -q_2 \tilde{y}^2 + q_0, \quad \text{and} \quad l_1 = \frac{\operatorname{Re} d_j - l_0}{\operatorname{Im} d_j}, \quad (5.11)$$

where l_1 follows directly from (5.10a), l_0 is obtained by substituting the value of l_1 given in (5.10c) into (5.10b), and \tilde{y} follows from substituting the value of l_0 given in (5.11) into l_1 in (5.11) (so that l_1 now only has \tilde{y} as an unknown), and then substituting this version of l_1 into (5.10c), which results in a quadratic equation in \tilde{y} . Thus, if $q(y)$ is a sufficiently accurate local model of $\partial W(A)$, it follows that

$$\bar{\theta}_{\text{Opt}} \approx \arctan l_1. \quad (5.12)$$

While [Fie81, Theorem 3.3] can be used to compute the (normalized) curvature at b_* , recall from Section 2 that its assumptions may not always hold. However, $q(y)$ can also be used to estimate the normalized curvature of $\partial W(A)$ at b_* :

$$\mu_{\text{est}} := \frac{1}{2q_2 \gamma}, \quad (5.13)$$

as the osculating circle of $q(y)$ at $y = 0$ has radius $\frac{1}{2}q_2$. This estimate will be useful in our third algorithm given in Section 6, which is a hybrid that (typically) begins by running Algorithm 2 but automatically switches to Algorithm 1 once it detects that the cutting-plane approach will be (much) less efficient.

In terms of implementation, if b_* is not on the positive real axis, we can simply first rotate all the points so that it then is, compute the rotated version of $\bar{\theta}_{\text{Opt}}$, and then rotate everything back. Similarly, if b_j is not in the upper half of the complex plane, we simply flip the problem, compute the flipped version of $\bar{\theta}_{\text{Opt}}$, and then flip back. In inexact arithmetic, we cannot expect that the optimal cut will pass through d_j exactly, and so rounding error may cause \hat{c}_{j+1} to be

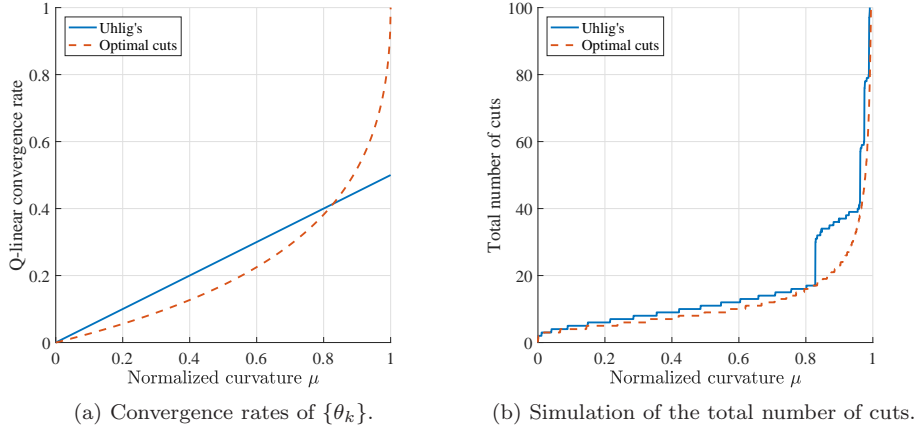


Figure 3: Left: the convergence rates (of the angles) for Uhlig's procedure and optimal cuts, respectively given by Theorems 4.9 and 5.4, are plotted. Right: via a trigonometric simulation of Example 4.5, we show the total number of cuts required to sufficiently refine the region of $\partial W(A)$ between b_j and b_* , where $\theta_j = \frac{\pi}{4}$ and $\text{tol}=1\text{e-}14$.

computed such that $|\hat{c}_{j+1}| \approx r$ but $|\hat{c}_{j+1}| > r(1 + \tau_{\text{tol}})$ still holds. As this rounding error would cause this second corner to also be subsequently refined, we first perturb d_j such that it is a tiny bit closer to b_j , i.e., we replace it with $(1 - \delta)d_j + \delta b_j$ for some small value of $\delta \in (0, 1)$.

In Fig. 3a, the convergence rates given by Theorems 4.9 and 5.4 are plotted for all possible values of μ . The rate for Uhlig's method is worse for normalized curvatures up to $\mu \approx 0.8283$, after which the optimal-cut strategy's rate becomes higher. For Fig. 3b, we show the total number of cuts needed by both approaches in order to sufficiently refine $\partial W(A)$ at an outermost point. With this perspective, we see that Uhlig's method actually becomes significantly worse than the optimal-cut procedure for normalized curvatures between $\mu \approx 0.8384$ and $\mu \approx 0.9610$, with Uhlig's method requiring up to almost double the number of cuts. In fact, Uhlig's method is typically always more expensive, though the differences are much smaller for other normalized curvature values. In Section 7, we show that our simulation in Fig. 3b accurately reflects what happens when using actual problems. Again, as $\mu \rightarrow 1$, the total costs of both methods blow up, in line with Theorem 4.1.

6 A hybrid algorithm

We now describe a hybrid algorithm whose main ingredients are Algorithms 1 and 2; as such, we forgo providing pseudocode and just describe it at a high level. The key ideas are that (a) we can predict when it is more efficient to use Algorithm 1 over Algorithm 2 or vice-versa, and (b) when Algorithm 2 is chosen, we can also algorithmically determine on the fly when it would likely be better to switch back to the level-set approach.

As motivated in Section 3, it is reasonable to assume that Algorithm 1 will often only require a single eigenvalue computation with $R_\gamma - \lambda S$. Meanwhile, Algorithm 2 only requires extremal eigenvalue computations with $H(\theta)$, and data like that shown in Fig. 3b provide good estimates of the total number of cuts that will be needed to compute $r(A)$ depending on the value of μ at outermost points. By doing benchmarking, e.g., as done in Table 1, we can construct look-up tables to determine for a given dimension how many eigenvalue computations we can do with $H(\theta)$ for the price of a single eigenvalue computation with $R_\gamma - \lambda S$. Thus, we can predict which approach will be faster. If μ is, say, less than 0.83, then very few cuts will be needed by Algorithm 2 and so it is likely to be faster than Algorithm 1 for all but the smallest values of n . Per Table 1, if $n \geq 800$, Algorithm 2 can incur about 100 cuts while still being faster

than Algorithm 1, and so Algorithm 2 will be faster for almost any normalized curvature value μ not too close to one (where the cost blows up). However, since we do not know the μ value(s) *a priori*, this motivates our second technique of how to dynamically decide when to switch back to Algorithm 1.

Suppose that our hybrid method starts the computation with Algorithm 2, based on the criteria discussed above. If, where $r(A)$ is attained, $\mu = 1$ or close to it, any cutting-plane method will become extremely expensive when computing $r(A)$ to more than just a few digits. To avoid this, one could set a small fixed limit on the total number of cuts that can be performed before halting Algorithm 2 and switching to Algorithm 1. When switching, Algorithm 1 will be warm started using the angle computed in line 5 of Algorithm 2. If this corresponds to a globally outermost point, Algorithm 1 will immediately verify this via a single eigenvalue computation with $R_\gamma - \lambda S$ and terminate. However, our optimal-cut strategy provides a more sophisticated way to determine when to switch (if at all). Once optimal cuts are being applied, μ_{est} from (5.13) estimates the value of μ at the corresponding locally outermost point in $W(A)$. If μ_{est} is very close to 1 and $r_{\text{ub}}(A, \mathcal{P}_j) - \gamma$ is not too large, indicating that μ_{est} is indeed likely a good estimate for μ , we can immediately switch to Algorithm 1. Furthermore, inside Algorithm 2, the current value of μ_{est} can be used to estimate how many more cuts will be needed before convergence is obtained. This prediction can then be compared with the look-up table data to dynamically set the limit on the total number of cuts allowed before switching.

Although our hybrid algorithm requires a one-time offline tuning phase (since the look-up table is likely hardware and software dependent), it can be particularly advantageous for applications where the numerical radius is being optimized. By detecting how μ changes as the field of values evolves, our hybrid method can automatically get the best of both algorithms, while avoiding the worst of both. Initially, it will likely only use Algorithm 2, which can be substantially faster. But as the parametric matrix becomes closer to a disk matrix, which again, often happens during optimization, it will start automatically falling back to Algorithm 1, thus avoiding the cost blow-ups that occur for cutting-plane approaches when μ is too close to 1.

7 Numerical validation

We implemented Algorithms 1 and 2 and compared them to earlier methods as well as each other. For lack of space, we forgo benchmarking our hybrid algorithm, though its benefits should be clear. For each problem, all computed estimates for $r(A)$ agreed to at least 14 digits, so we only show cost comparisons. Implementations of our methods will be added to ROSTAPACK [Mit].

We begin by comparing Algorithm 1 to `numr`, Mengi's MATLAB implementation⁵ of his level-set method with Overton. Per Table 3, Algorithm 1 ranged from 2.9–6.8 times faster than `numr`, with it indeed only needing a single eigenvalue computation with $R_\gamma - \lambda S$ for all the problems except $n = 200$ (where it needed two). With optimization disabled, our BBBS-like iteration using (2.5) was also faster than `numr`, though not nearly as fast as Algorithm 1.

Moving to Algorithm 2, recall that the simulation illustrated in Fig. 3b indicates that our optimal-cut strategy should be appreciably faster than Uhlig's method for normalized curvatures $\mu \in (0.8384, 0.9610)$, approximately. We now verify this by running codes on actual instances of Example 4.5. Note that we use Example 4.5, as opposed to other test problems, precisely because Example 4.5 allows us to create test problems with any normalized curvature. In Fig. 4a, we indeed see that the total costs in practice for Uhlig's method and Algorithm 2 agree nearly identically with the simulated costs in Fig. 3b. Moreover, this also verifies that our procedure to estimate the optimal cut, from Section 5.3, is sufficiently accurate to realize the convergence rate given in Theorem 5.4. In Fig. 4b, we repeat the experiment with rotated versions of same problems, to test the methods when symmetry of $W(A)$ is not exploited; here we see that the total costs about double, as expected, while the optimal-cut strategy is still up to about twice as fast as Uhlig's procedure.

⁵ Available at <http://home.ku.edu.tr/~emengi/software/robuststability.html>.

Table 3: For dense random A matrices, the costs of Algorithm 1 and the BBBS-like method of Mengi and Overton (MO) are shown. We tested Algorithm 1 with optimization (Opt.) and without optimization (MP, for midpoints only).

n	# of $\text{eig}(H(\theta))$			# of $\text{eig}(R_\gamma, S)$			Time (sec.)		
	Alg. 1		MO	Alg. 1		MO	Alg. 1		MO
	Opt.	MP		Opt.	MP		Opt.	MP	
100	7	5	34	1	4	5	0.1	0.2	0.3
200	9	7	38	2	4	6	0.8	1.4	2.3
300	16	5	26	1	4	5	1.4	4.4	6.0
400	9	10	43	1	5	7	3.0	13.9	19.6
500	5	4	54	1	3	7	4.2	12.4	28.6
600	6	5	36	1	4	5	7.9	28.5	37.2

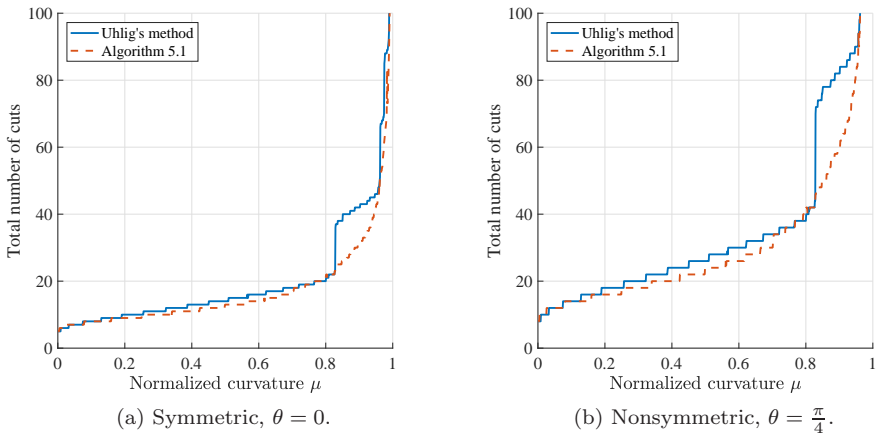


Figure 4: Total number of cuts needed by our own implementations of Uhlig's method and Algorithm 2 to compute $r(A)$ of instances of Example 4.5, where $A = zI + \mu K_5$ and only λ_{\max} of $H(\theta)$ is used. Left: $W(A)$ is a disk of radius μ centered at $z = (1 - \mu)$, and both codes automatically exploit the real-axis symmetry. Right: the cost to compute $r(e^{i0.25\pi} A)$ is shown, i.e., $W(A)$ rotated into the upper right quadrant so symmetry is no longer exploited, and so the number of cuts about doubles.

Finally, we compare our improved level-set and cutting-plane methods. For these experiments, per Remark 2.6, we set Algorithm 2 to also add the supporting hyperplane for λ_{\min} on every cut. We chose to use `eig` for all computations with $H(\theta)$, for both Algorithms 1 and 2, partly for simplicity but also because while `eigs` often works well on $H(\theta)$, we observed it was not always reliable for computing eigenvalues of A . That being said, for cutting-plane methods, note that obtaining eigenvalues of A is not so critical, since (a) per our new theory, the cutting-plane methods will converge Q-superlinearly for normal matrices, and (b) the eigenvalues of A are otherwise only used to guess a good rotation of the initial polygonal approximation of $W(A)$.

For test problems of dimension $n = 320, 640$, and 1280 , we reused Uhlig's Gear, Grcar, and FM examples from [Uhl09, Section 3], and added complex random matrices, which we call `randn`, and for $\mu = 0.999$, $A = e^{i0.25\pi}((1 - \mu)I + \mu K_n)$, which we call Nearly Disk and is a variant of the nonsymmetric examples we used for Fig. 4b. The results of our comparison are given in Table 4. Over all the problems, we again see that Algorithm 1 usually only requires a single computation with $R_\gamma - \lambda S$ (and for these problems, never more than two), again verifying that our level-set approach is well optimized in terms of efficiency. Meanwhile, we observe that the overall cost of Algorithm 2 is indeed highly correlated with the normalized curvature of the respective test

Table 4: The respective costs of Algorithms 1 and 2 are shown. The normalized curvatures μ are also shown, which were computed via [Fie81, Theorem 3.3].

Problem	n	μ	# of calls to <code>eig</code> (\cdot)		Time (sec.)	
			Alg. 1		Alg. 2	Alg. 1
			$H(\theta)$	$R_\gamma - \lambda S$	$H(\theta)$	Alg. 2
Gear	320	0.000	1	1	5	1.4
Gear	640	0.000	2	1	3	21.4
Gear	1280	0.000	2	1	4	343.2
Grcar	320	0.654	45	2	30	3.0
Grcar	640	0.654	82	2	31	38.2
Grcar	1280	0.654	161	2	30	576.4
FM	320	0.185	9	1	20	1.1
FM	640	0.184	6	1	18	10.0
FM	1280	0.183	9	1	20	88.0
<code>randn</code>	320	0.758	5	1	41	1.5
<code>randn</code>	640	0.866	17	2	73	26.7
<code>randn</code>	1280	0.797	18	2	61	232.5
Nearly Disk	320	0.999	2	1	511	2.0
Nearly Disk	640	0.999	2	1	511	17.2
Nearly Disk	1280	0.999	2	1	531	167.7
						429.1

problems, per our theoretical analysis. On Gear, where $\mu = 0$, Algorithm 2 is extremely fast, demonstrating Q-superlinear convergence. For Gear, Grcar, FM, and `randn`, Algorithm 2 is 2 to 111 times faster than Algorithm 1 since none of these problems have normalized curvatures very close to 1. Note that if the cuts in Algorithm 2 had been done via `eigs` instead of `eig`, these performance gaps would likely be even wider. Finally, for Nearly Disk, where $\mu = 0.999$, Algorithm 2 is very slow as predicted, with our level-set approach now being 2.6 to 5.3 times faster. Clearly, our benchmarks in Table 4 underscore the benefits of our hybrid algorithm.

8 Conclusion

We have established the first rate-of-convergence results for both Mengi and Overton’s level-set approach and Uhlig’s cutting-plane method for computing the numerical radius, while also introducing three improved algorithms. Our enhancements to each approach resulted in Algorithm 1 and Algorithm 2, both of which are significantly faster than the earlier methods. Crucially, our new analysis explains why cutting-plane methods are sometimes exceptionally fast and sometimes exceptionally slow, which in turn motivated our hybrid algorithm combining both level-set and cutting-plane techniques. By dynamically detecting when to switch between these two approaches, our hybrid algorithm remains efficient across all numerical radius problems.

References

- [BB90] S. Boyd and V. Balakrishnan. A regularity result for the singular values of a transfer matrix and a quadratically convergent algorithm for computing its L_∞ -norm. *Systems Control Lett.*, 15(1):1–7, 1990.
- [BBMX02] P. Benner, R. Byers, V. Mehrmann, and H. Xu. Numerical computation of deflating subspaces of skew-Hamiltonian/Hamiltonian pencils. *SIAM J. Matrix Anal. Appl.*, 24(1):165–190, 2002.
- [Ben02] I. Bendixson. Sur les racines d’une équation fondamentale. *Acta Math.*, 25(1):359–365, 1902.
- [Ber65] C. A. Berger. A strange dilation theorem. *Notices Amer. Math. Soc.*, 12:590, 1965.
- [BLO03] J. V. Burke, A. S. Lewis, and M. L. Overton. Robust stability and a criss-cross algorithm for pseudospectra. *IMA J. Numer. Anal.*, 23(3):359–375, 2003.
- [BM19] P. Benner and T. Mitchell. Extended and improved criss-cross algorithms for computing the spectral value set abscissa and radius. *SIAM J. Matrix Anal. Appl.*, 40(4):1325–1352, 2019.

[BS90] N. A. Bruinsma and M. Steinbuch. A fast algorithm to compute the H_∞ -norm of a transfer function matrix. *Systems Control Lett.*, 14(4):287–293, 1990.

[BSV16] P. Benner, V. Sima, and M. Voigt. Algorithm 961: Fortran 77 subroutines for the solution of skew-Hamiltonian/Hamiltonian eigenproblems. *ACM Trans. Math. Software*, 42(3):Art. 24, 26, 2016.

[Bye88] R. Byers. A bisection method for measuring the distance of a stable matrix to unstable matrices. *SIAM J. Sci. Statist. Comput.*, 9:875–881, 1988.

[DHT14] T. A Driscoll, N. Hale, and L. N. Trefethen. *Chebfun Guide*. Pafnuty Publications, Oxford, UK, 2014.

[Fie81] M. Fiedler. Geometry of the numerical range of matrices. *Linear Algebra Appl.*, 37:81–96, 1981.

[HJ91] R. A. Horn and C. R. Johnson. *Topics in Matrix Analysis*. Cambridge University Press, Cambridge, 1991.

[HW97] C. He and G. A. Watson. An algorithm for computing the numerical radius. *IMA J. Numer. Anal.*, 17(3):329–342, June 1997.

[Joh78] C. R. Johnson. Numerical determination of the field of values of a general complex matrix. *SIAM J. Numer. Anal.*, 15(3):595–602, 1978.

[Kat82] T. Kato. *A Short Introduction to Perturbation Theory for Linear Operators*. Springer-Verlag, New York - Berlin, 1982.

[Kip51] R. Kippenhahn. Über den Wertevorrat einer Matrix. *Math. Nachr.*, 6(3-4):193–228, 1951.

[Kre62] H.-O. Kreiss. Über die Stabilitätsdefinition für Differenzengleichungen die partielle Differentialgleichungen approximieren. *BIT*, 2(3):153–181, 1962.

[Küh15] W. Kühnel. *Differential Geometry: Curves—Surfaces—Manifolds*, volume 77 of *Student Mathematical Library*. American Mathematical Society, Providence, RI, third edition, 2015. Translated from the 2013 German edition by Bruce Hunt, with corrections and additions.

[Lan64] P. Lancaster. On eigenvalues of matrices dependent on a parameter. *Numer. Math.*, 6:377–387, 1964.

[LO20] A. S. Lewis and M. L. Overton. Partial smoothness of the numerical radius at matrices whose fields of values are disks. *SIAM J. Matrix Anal. Appl.*, 41(3):1004–1032, 2020.

[Mit] T. Mitchell. ROSTAPACK: RObust STAbility PACKage. <http://timmitchell.com/software/ROSTAPACK>.

[Mit19] T. Mitchell. Fast interpolation-based globality certificates for computing Kreiss constants and the distance to uncontrollability. e-print arXiv:1910.01069, arXiv, October 2019. math.OC.

[Mit20] T. Mitchell. Computing the Kreiss constant of a matrix. *SIAM J. Matrix Anal. Appl.*, 41(4):1944–1975, 2020.

[MO05] E. Mengi and M. L. Overton. Algorithms for the computation of the pseudospectral radius and the numerical radius of a matrix. *IMA J. Numer. Anal.*, 25(4):648–669, 2005.

[NW99] J. Nocedal and S. J. Wright. *Numerical Optimization*. Springer, New York, 1999.

[OW95] M. L. Overton and R. S. Womersley. Second derivatives for optimizing eigenvalues of symmetric matrices. *SIAM J. Matrix Anal. Appl.*, 16(3):697–718, 1995.

[Pea66] C. Pearcy. An elementary proof of the power inequality for the numerical radius. *Michigan Math. J.*, 13:289–291, 1966.

[TE05] L. N. Trefethen and M. Embree. *Spectra and Pseudospectra: The Behavior of Nonnormal Matrices and Operators*. Princeton University Press, Princeton, 2005.

[TY99] B.-S. Tam and S. Yang. On matrices whose numerical ranges have circular or weak circular symmetry. *Linear Algebra Appl.*, 302–303:193–221, 1999. Special issue dedicated to Hans Schneider (Madison, WI, 1998).

[Uhl09] F. Uhlig. Geometric computation of the numerical radius of a matrix. *Numer. Algorithms*, 52(3):335–353, 2009.

[Wat96] G. A. Watson. Computing the numerical radius. *Linear Algebra Appl.*, 234:163–172, 1996.